

Comparative whole genome analysis reveals re-emergence of typical human Wa-like and DS-1-like G3 rotaviruses after Rotarix vaccine introduction in Malawi

Chimwemwe Mhango^{1,2}, Akuzike Banda³, End Chinyama¹, Jonathan J. Mandolo^{1,2}, Orpha Kumwenda¹, Chikondi Malamba-Banda^{1,10,16,17}, Kayla G. Barnes¹, Benjamin Kumwenda², Kondwani Jambo^{1,4}, Celeste M. Donato^{5,6}, Mathew D. Esona⁷, Peter N. Mwangi⁸, A. Duncan Steele⁷, Miren Iturriza-Gomara⁹, Nigel A. Cunliffe^{10,11}, Valentine N. Ndze¹², Arox W. Kamng'ona^{1,2*}, Francis E. Dennis¹³, Martin M. Nyaga^{8#}, Chrispin Chaguzo^{10,14,15#}, Khuzwayo C. Jere^{1,10,11,17#*}

¹Malawi-Liverpool-Wellcome Clinical Research Program, Kamuzu University of Health Sciences, Blantyre, Malawi

²Department of Biomedical Sciences, School of Life Sciences and Allied Health Professions, Kamuzu University of Health Sciences, Blantyre, Malawi

³Department of Computer Science, Faculty of Science, University of Malawi

⁴Department of Clinical Sciences, Liverpool School of Tropical Medicine, Liverpool, United Kingdom

⁵Enteric Diseases Group, Murdoch Children's Research Institute, 50 Flemington Road, Parkville, Melbourne 3052, Australia

⁶Department of Paediatrics, the University of Melbourne, Parkville 3010, Australia

⁷Diarrhoeal Pathogens Research Unit, Sefako Makgatho Health Sciences University, Medunsa 0204, Pretoria, South Africa

⁸Next Generation Sequencing Unit and Division of Virology, Faculty of Health Sciences, University of Free State, Bloemfontein 9300, South Africa.

⁹Centre for Vaccine Innovation and Access, Program for Appropriate Technology in Health (PATH), Geneva 1218, Switzerland

¹⁰Institute of Infection, Veterinary and Ecological Sciences, University of Liverpool, UK

¹¹NIHR Health Protection Research Unit in Gastrointestinal Infections, University of Liverpool, United Kingdom.

¹²Faculty of Health Sciences, University of Buea, P.O. Box 63, Buea, Cameroon

¹³Department of Electron Microscopy and Histopathology, Noguchi Memorial Institute for Medical Research, University of Ghana

¹⁴Department of Epidemiology of Microbial Diseases, Yale School of Public Health, Yale University, New Haven, CT, USA

¹⁵NIHR Mucosal Pathogens Research Unit, Division of Infection and Immunity, University College London, London, United Kingdom

38 ¹⁶Department of Biological Sciences, Academy of Medical Sciences, Malawi University of
39 Science and Technology, Thyolo, Malawi

40 ¹⁷Department of Medical Laboratory Sciences, Faculty of Biomedical Sciences and Health
41 profession, Kamuzu University of Health Sciences, Blantyre, Malawi

42

43 #Contributed equally.

44 *To whom correspondence should be addressed: AWK: awkamngona@kuhes.ac.mw and KCJ:

45 Khuzwayo.Jere@liverpool.ac.uk

46

47 **Running title:** Sequence analysis of G3 rotaviruses from Malawi

48

Abstract

Genotype G3 rotaviruses rank among the most common rotavirus strains worldwide in humans and animals. However, despite a robust long-term rotavirus surveillance system from 1997 in Blantyre, Malawi, these strains were only detected from 1997 to 1999 and then disappeared and re-emerged in 2017, five years after the introduction of the Rotarix rotavirus vaccine. Here we analysed 27 whole genome sequences to understand how G3 strains re-emerged in Malawi. We randomly selected samples each month between November 2017 and August 2019 from stool samples of children hospitalised with acute diarrhoea at the Queen Elizabeth Hospital in Blantyre, Malawi. We found three genotypes namely G3P[4] ($n=20$), G3P[6] ($n=1$) and G3P[8] ($n=6$) associated with the re-emergence of G3 strains in Malawi post-Rotarix vaccine introduction. The identified genotypes co-circulated at different time points and were associated with three typical human G3 strains consisting of either a Wa-like or DS-1-like genetic constellation and reassortant strains possessing Wa-like and DS-1-like genetic backbones. Time-resolved phylogenetic trees demonstrated that the most recent common ancestor for each segment of the re-emerged G3 strains emerged between 1996 and 2012, possibly through introductions from outside the country due to the limited genetic similarity with G3 strains which circulated before their disappearance in the late 1990s. Further genomic analysis revealed that the reassortant DS-1-like G3P[4] strains acquired a Wa-like NSP2 genome segment (N1 genotype) through intergenogroup reassortment; an artiodactyl-like VP3 through intragenogroup interspecies reassortment; and VP6, NSP1 and NSP4 segments through intragenogroup reassortment likely before importation into Malawi. Additionally, the re-emerged G3 strains contain amino acid substitutions within the antigenic regions of the VP4 proteins which could potentially impact the binding of rotavirus vaccine-induced antibodies. Altogether, our findings shows that multiple rather than a single genotype have driven the re-emergence of G3 strains likely from other countries highlighting the role of human mobility and genome reassortment events in the dissemination and evolution of rotavirus strains in Malawi necessitating the need for long-term genomic surveillance of rotavirus in high disease burden settings to inform disease prevention and control.

Key words: Rotavirus, G3 strains, Whole-genome sequencing, Sub-Saharan Africa, Malawi, Phylodynamic, Reassortment, Importation, Genotype re-emergence, Rotarix vaccine

1 Introduction

2 Childhood vaccination remains the most effective public health intervention against rotavirus
3 gastroenteritis (Chandran et al. 2010). Despite the introduction of rotavirus vaccines in 114
4 countries globally (“VIEW-Hub by IVAC” n.d.), rotavirus remains the leading etiological agent
5 of acute gastroenteritis in children (Clark et al. 2017), and is associated with approximately
6 128,500 deaths per annum among children <5 years old worldwide (Troeger et al. 2018). To
7 reduce the global burden of gastroenteritis in children, the World Health Organisation (WHO)
8 has pre-qualified the use of four rotavirus vaccines: Rotarix (GlaxoSmithKline, Rixensart,
9 Belgium), RotaTeq (Merck and Co., Whitehouse Station, NJ, USA), ROTAVAC (Bharat
10 Biotech, India) and ROTASIIL (Serum Institute of India Pvt. Ltd., India) (Kirkwood and Steele
11 2018). These vaccines are highly effective at preventing mortality, hospitalizations, and severe
12 rotavirus gastroenteritis episodes in high-income settings, although lower effectiveness has been
13 reported in low- and middle-income countries (Henschke et al. 2022; Cates, Tate, and Parashar
14 2022; Saha et al. 2021). The Rotarix vaccine was introduced into Malawi’s Extended Program
15 of Immunisation (EPI) in October 2012, and by 2016, over 99% of vaccine coverage was
16 reached (Bennett et al. 2021). The Rotarix vaccine has demonstrated relatively modest
17 effectiveness in Malawi (31.7 to 70.6%) during programmatic use compared with that observed
18 in high income settings, although effectiveness against severe rotavirus gastroenteritis in the first
19 year of life is higher against homotypic (70%) compared with heterotypic (40 to 60%) strains
20 (Bar-Zeev et al. 2016).

21
22 Rotavirus has a double-stranded RNA genome and belongs to the *Reoviridae* family. Its genome
23 contains eleven segments that encode six structural proteins (VP1-VP4, VP6 and VP7) and up to
24 six non-structural proteins (NSP1-NSP5/6) (Estes et al. 2007). To fully characterise rotavirus
25 strains, a whole genome classification system was devised to assign genotypes to each genome
26 segment (Matthijnssens, Ciarlet, Rahman, et al. 2008). To date, 41 G, 57 P, 31 I, 27 R, 23C, 23
27 M, 38 A, 27 N, 27 T, 31 E, and 27 H genotypes have been assigned for the VP7, VP4, VP6, VP1,
28 VP2, VP3, NSP1, NSP2, NSP3, NSP4 and NSP5 genome segments, respectively
29 (<https://rega.kuleuven.be/cev/viralmetagenomics/virus-classification>). While most infections are
30 associated with a single genotype, coinfections with rotavirus strains of different genotypes are

31 also common, which provides favourable conditions for generating progeny viruses with
32 reassortant genomic segments. These genomic reassortment events together with high mutation
33 rates arising from an error-prone RNA polymerase (VP1) that lacks proof-reading mechanisms
34 are the main mechanisms of evolution for rotaviruses (Estes et al. 2007).

35
36 Clinically, genotypes G1P[8], G2P[4], G3P[8], G4P[8], G9P[8] and G12P[8] are the most
37 common rotavirus strains associated with diarrhoea in under five children globally (Dóro et al.
38 2014). The distribution of these and other rotavirus genotypes vary by geographical location and
39 appear to depend on the rotavirus vaccination status and the vaccine used in a particular region
40 (Donato et al. 2022). Before global introduction of rotavirus vaccines across the continents,
41 G1P[8] genotypes were the predominant strains detected globally (Bányai et al. 2012). However,
42 G2P[4] strains have been predominant in some countries using Rotarix rotavirus vaccine while
43 the G12P[8] genotype has been commonly detected in some countries using RotaTeq rotavirus
44 vaccine (Rocz-Farkas et al. 2018; Hungerford et al. 2019; Carvalho-Costa et al. 2019; Vizzi et
45 al. 2017; Degiuseppe and Stupka 2018). The detection rates of G3 strains and other sporadically
46 circulating genotypes has increased especially in countries using Rotarix rotavirus vaccine
47 globally (Carvalho-Costa et al. 2019; Wahyuni et al. 2021; Rocz-Farkas et al. 2018). While
48 genotype G3 was not common in the African continent before rotavirus vaccine introduction,
49 these strains have been reported in several African countries post-vaccination (Mhango et al.
50 2020; Mwanga et al. 2020; João et al. 2020). Our previous work reported the prevalence of
51 rotavirus strains circulating in Blantyre, Malawi from 1997 to 2019 (Mhango et al. 2020). We
52 showed that genotypes G1, G4 and G8 were frequently detected before Rotarix rotavirus vaccine
53 introduction, whereas G1, G2, G3 and G12 genotypes were more common during the vaccine
54 era (Mhango et al. 2020). Although G3 strains were last detected between 1997 to 1999 before
55 their re-emergence in 2017 after nearly two decades, they became the most predominant
56 rotavirus strains in Blantyre, Malawi by the end of 2019 following their re-emergence in 2017
57 (Mhango et al. 2020).

58
59 Although G3 rotaviruses are associated with a wide range of host species and “P” genotype
60 combinations (Martínez-Laso et al. 2009; Matthijnsens et al. 2006), it’s unknown whether the
61 re-emerged G3 rotaviruses belong to a single genotype, particularly P[8] which constitutes the

62 majority of human-associated strains (Matthijnsens, Ciarlet, Heiman, et al. 2008). It's also
63 unknown whether the genetic background of the re-emerged G3 strains in Malawi possess a
64 typical human or equine-like VP7 genome segment and DS-1-like genetic backbone as recently
65 seen in various settings globally after the introduction of rotavirus vaccines (Komoto et al. 2018;
66 Cowley et al. 2016; Dóro et al. 2016; Esposito et al. 2019; Arana et al. 2016; Luchs et al. 2019).
67 To address these questions, we generated whole genome sequences of G3 strains collected
68 through our robust and long-term hospital-based rotavirus surveillance in Blantyre, Malawi to
69 investigate their genomic epidemiology and evolution in Malawi and broader international
70 context. Our findings show that re-emergence of G3 rotavirus strains was driven by multiple
71 genotypes, including reassortant strains, with highest genetic similarity with strains from other
72 countries, highlighting the impact of importation events as a mechanism for reseeding the strains
73 in the post-vaccination era following their nearly two decades hiatus in Malawi.

74 Results

75 G3 rotaviruses strains became the predominant genotype in Malawi after
76 their re-emergence in November 2017

77 Active rotavirus surveillance has been on-going at QECH from 1997 of which a wide diversity
78 of rotavirus strains has been reported from stools collected from children presenting with
79 diarrhoea during weekdays (Mhango et al. 2020). G3 strains were last detected in 1999 (0.02%
80 of total genotypes; 4/166) and re-emerged in November 2017, five years after the introduction of
81 the rotavirus vaccine. By 2018, G3 strains had completely replaced G1 and G2 strains as the
82 most commonly detected rotavirus strains in Malawi (Mhango et al. 2020). Genotype G3P[4]
83 strains re-emerged first in 2017 and were detected at high frequencies (12.3 to 36.3% of all
84 genotypes), G3P[6] strains were sporadically detected (1.2%) between September 2018 to March
85 2019 where as G3P[8] were first detected in December 2018 and predominated in 2019 (27.2%
86 of all genotypes) (Mhango et al. 2020). To gain insight into the evolutionary events that led to
87 the re-emergence of G3 rotaviruses in Malawi, full length nucleotide sequences for 30 G3 strains
88 that circulated before and after vaccine introduction periods were generated and analysed (Figure
89 1 and Supplementary Table S1).

90 Re-emergent G3 rotaviruses in Malawi were associated with four variants
91 G3 strains are associated with a wider host range which predisposes them to reassortment events
92 as well as emergence of unusual G3 variants (Martínez-Laso et al. 2009; Matthijnssens et al.
93 2006). Normally, the inner capsid genome segments of human rotaviruses have either a Wa-like
94 (I1-R1-C1-M1-A1-N1-T1-E1-H1), DS-1-like (I2-R2-C2-M2-A2-N2-T2-E2-H2) or AU-1-like
95 (I3-R3-C3-M3-A3-N3-T3-E3-H3) genotype constellation. To gain insights in the genotype
96 constellations of the G3 variants that re-emerged and predominated between 2017 to 2019 in
97 Blantyre, Malawi, we analysed the whole genome sequences (WGS) of 27 representative G3
98 strains that re-emerged to determine the genomic constellations of the viruses. WGS analysis
99 revealed that sixteen G3P[4] (80%, $n=20$) strains had a pure DS-1-like genotype constellation
100 (Table 1). The only G3P[6] strain that was sequenced also had a pure DS-1-like genotype
101 constellation (Table 1). In contrast, the three G3P[8] strains detected from 1997 to 1999 (33.3%,
102 $n=9$) before rotavirus vaccine introduction and six from 2018 to 2019 (66.6%, $n=9$) during the
103 rotavirus vaccine era in Malawi had the Wa-like genotype constellation (Table 1). Unexpectedly,
104 four G3P[4] (20%, $n=20$) strains that were detected towards the end of 2018 had a mosaic
105 genotype constellation consisting of a core DS-1-like backbone but with an N1 NSP2 Wa-like
106 rather than an N2 DS-1-like genome segment. We therefore classified these atypical viruses as
107 reassortant DS-1-like G3P[4] strains (Table 1). Thus, a total of four genotype G3 variants
108 circulated between 2017 and 2019, namely the typical DS-1-like strains (G3P[4] and G3P[6]),
109 reassortant DS-1-like strains (G3P[4]) and Wa-like strains (G3P[8]), of which the later two co-
110 circulated in late 2018.

111
112 Genome segments of segmented viruses tend to have evolutionary rates that vary per segment.
113 This coupled with reassortment events tend to increase genomic diversity of segmented viruses.
114 To assess the genomic diversity within the re-emergent G3 variants, we placed the VP7, VP4 and
115 inner capsid genome segments for DS-1-like G3 variants into global context based on the
116 lineages defined by Sadiq et al. and Agbemabiese et al. (Agbemabiese et al. 2019; Sadiq et al.
117 2019). We could not do the same for the inner capsid segments of the Wa-like strains since there
118 is no known lineage framework for Wa-like genome segments. WGS analysis revealed a wider
119 genomic diversity (1 to 4) per genome segment for the re-emerged four G3 variants
120 (Supplementary Table S2). The highest diversity was observed within VP4 while the lowest was

121 seen in VP7 (Supplementary Table S2). However, we also observed within lineage variation for
122 DS-1-like variants (VP1, VP2, VP3, and NSP3) having up to 2, while NSP5 had up to three
123 unique clusters within the same lineage (Supplementary Figure S3). Although we only identified
124 four variants associated with the G3 rotavirus strains, the association of the G3 strains with
125 multiple lineages suggest a high genomic diversity of the re-emerged G3 strains circulated in
126 Blantyre, Malawi between 2017 and 2019.

127 Re-emergent G3 strains were genetically distinct from previous and co- 128 circulating rotaviruses in Malawi

129 Naturally, reassortment events are common within rotaviruses when multiple strains infect a
130 single host. Since our present findings revealed a co-circulation of Wa-like and DS-1-like G3
131 strains late in 2018; we therefore explored the possibility that the reassortant DS-1-like G3P[4]
132 strains acquired a Wa-like NSP2 genome segment through coinfections of Wa-like and DS-1-like
133 strains that co-circulated in Malawi. We constructed a Maximum likelihood phylogenetic tree for
134 all Malawian Wa-like NSP2 (N1) genome segment to explore their genetic relationship to the
135 NSP2 of the reassortant DS-1-like G3P[4] strains. The phylogenetic analysis revealed that the
136 Wa-like NSP2 genome segment (N1 genotype) of the reassortant DS-1-like G3P[4] strains
137 formed a separate monophyletic cluster from the N1 NSP2 genome segments that were
138 associated with co-circulating Wa-like G3P[8] and other locally detected non-G3 strains
139 (Supplementary Figure S2). The NSP2 genome segment of the reassortant DS-1-like G3P[4] and
140 other co-circulating Wa-like Malawian strains differed by 20-23 SNPs within the NSP2 ORF
141 sequence. These findings suggested that the NSP2 genome segment of the re-emerged G3 strains
142 was not acquired from strains circulating in Malawi, especially after the re-emergence of the G3,
143 as these could have most likely been detected by our rotavirus surveillance system.

144
145 Previous WGS work in Malawi revealed a circulation of non-G3 genotypes on either a Wa-like
146 or a DS-1-like genomic constellation (Jere et al. 2018). Considering the segmented nature of
147 rotaviruses, we conducted a genome segment specific time resolved phylogenetic analysis to
148 assess the genomic similarity of the re-emerged strains to locally detected co-circulating non-G3
149 Wa-like or DS-1-like rotaviruses in Malawi. When we employed the time tree analysis to
150 compare the nucleotide sequences of the VP4 and nine backbone genome segments, we observed

151 that the pre- and post-vaccine G3 strains formed separate monophyletic clades from the co-
152 circulating non-G3 Wa-like and DS-1-like strains (Figure 2 and Supplementary Figure S1).
153 These findings suggested that the re-emerged G3 strains did not evolve from or acquire their
154 genome segments from the other co-circulating non-G3 rotaviruses raising the possibility of new
155 introduction of these strains into Malawi.

156
157 When we focused on the clustering patterns of the G3 strains, we identified two distinct
158 populations for genome segments encoding both structural and non-structural proteins for
159 Malawian G3P[4] strains that formed separate monophyletic clades. The monophyletic clades for
160 the DS-1-like G3P[4] strains clustered away from the reassortant DS-1-like G3P[4] strains in
161 VP1, VP2, VP4, NSP3 and NSP5 encoding genome segments (Figure 2). Even though the
162 reassortant DS-1-like G3P[4] strains emerged after the DS-1-like G3P[4] and shared similar
163 NSP1, NSP4 and VP6 genome segments, the tMRCA of the NSP3, NSP5, VP1, VP2 and VP4
164 genome segments for the reassortant DS-1-like G3P[4] strains (ranging from 2001 – 2010)
165 (Table 2) and that of the DS-1-like G3P[4] strains (ranging from 2001 – 2008) (Table 2) varied
166 considerably across the respective segments. When we looked at the estimated mutation rates for
167 each of the genome segments (NSP3, NSP5, VP1, VP2, VP3 and VP4) (2.52×10^{-4} to 1.67×10^{-3}
168 nucleotide substitutions per site per year) (Table 2), the number of single nucleotide
169 polymorphisms (SNPs) and the time between the initial emergence of the two G3P[4] variants,
170 we concluded that there was not enough time for these specific genome segments of reassortant
171 DS-1-like G3P[4] to have evolved from the DS-1-like genome segments. Thus, these data
172 suggested that the DS-1-like G3P[4] and reassortant DS-1-like G3P[4] strains did not share an
173 immediate common ancestor and that the reassortant DS-1-like G3P[4] strains were introduced
174 independently already having a reassortant NSP2 genome segment from a source where DS-1-
175 like G3P[4] strains similar to those detected in Blantyre, Malawi during this period were also
176 circulating.

177 Re-emerged G3 strains resembled typical human rotaviruses likely
178 imported into Malawi

179 Human G3 rotaviruses have been detected at higher frequencies globally during the past decade
180 with the majority possessing equine-like rotavirus genome segments. While the present study G3

181 strains had either a DS-1-like or Wa-like genomic constellation, the origins of the genome
182 segments were unclear. To determine the potential host origins of the re-emerged G3 strains, we
183 performed a maximum likelihood phylogenetic analysis for the VP7 genome segment of the
184 Malawian and globally detected G3 strains (2010 - 2020). Maximum likelihood analysis revealed
185 that the genome segments encoding VP7 for all Malawian G3 strains clustered together with
186 those of the typical human G3 strains that were detected from various countries across the globe
187 (Figure 3). Except for the VP3, the rest of the genome segments clustered together with genome
188 segments characterised from other human rotaviruses (Supplementary Figure S3). The VP3 (M2)
189 genome segments of the reassortant G3P[4] strains clustered together with M2 genome segments
190 commonly characterised in ruminant animals (Figure 4b). This suggested that intragenogroup
191 reassortment events between human rotaviruses and strains that circulate in Artiodactyla order
192 were part of the evolutionary events that led to the emergence of the reassortant DS-1-like
193 G3P[4] strains.

194
195 We then looked at the geographical origin of the genome segments associated with G3
196 rotaviruses circulating in Malawi. Maximum likelihood analysis revealed that all VP7 genome
197 segments associated with strains possessing a DS-1-like genetic backbone (G3P[4], reassortant
198 G3P[4] and G3P[6]) shared a high nucleotide sequence similarity with only 4 to 6 SNPs
199 observed within the ORF to contemporary G3P[4] strains characterised in the middle east Asia,
200 Pakistan (Figure 3 and Supplementary Figure S3). In contrast, the VP7 genome segment of Wa-
201 like (G3P[8]) strains clustered together with and only had 5 to 7 SNPs within the ORF to
202 contemporary G3P[8] strains characterised in the far east Asia (Japan and Thailand) (Figure 3
203 and Supplementary Figure S3). The rest of the DS-1-like G3P[4] genome segments clustered
204 together with isolates from the Asian continent with a highest nucleotide sequence similarity
205 (99.40% to 99.70%) observed against contemporary G3P[4] strains that were detected in
206 Pakistan (Figure 4 and Supplementary Figure S3). With the exception of NSP1 and VP4, the
207 genome segments for the DS-1-like G3P[6] study strain had a similar clustering pattern to our
208 study DS-1-like G3P[4] strains which showed a high nucleotide sequence similarity to African
209 (Mozambique, Zambia, Zimbabwe and South Africa) DS-1-like isolates (Supplementary Figure
210 S3). To the contrary, we observed two clustering patterns of the re-emerged reassortant DS-1-
211 like G3P[4] strains in Malawi depending on the genome segment. While NSP1, NSP4 and VP6

212 showed a high nucleotide sequence identity to Asian (Pakistan) isolates, similar to the DS-1-like
213 G3P[4] strains, their NSP2, NSP5, VP1, VP2 and VP4 showed a high nucleotide sequence
214 identity (99.51% to 99.70%) to similar genome segments characterised in Europe (Czech
215 Republic) (Figure 4, and Supplementary Figure S3). On the other hand, the Wa-like G3P[8]
216 genome segments showed similarity to Wa-like segments for non-G3 strains characterised from
217 the African (Zimbabwe, South Africa, Mozambique, Kenya and Rwanda) and Wa-like G3P[8]
218 from the Asian (Japan, India and Indonesia) continents (Figure 4 and Supplementary Figure
219 S3.). Although the majority of these findings showed a high similarity to Asian countries, these
220 genome segments are widespread across the African, Asian, European, and potentially other
221 unsampled settings suggesting a potential for frequent cross border dissemination.

222 Reassortant DS-1-like G3P[4] likely emerged through multiple reassortment
223 events prior to their introduction into Malawi

224 As all genome segments for the reassortant DS-1-like G3P[4] did not cluster with those of the
225 other rotavirus strains that were circulating in Malawi, we used phylogenetic inferences for each
226 genome segment to determine the origin of the reassortant strains. Since the VP1, VP2, VP4,
227 NSP3 and NSP5 encoding genome segments of the reassortant DS-1-like G3P[4] were not
228 closely related to currently available strains in the GenBank, presumably due to dearth of
229 genomic rotavirus surveillance in many countries, we hypothesised that the reassortant DS-1-like
230 G3P[4] acquired these five genome segments from human rotaviruses that circulated from
231 unsampled locations. Our reassortant strains likely acquired their VP3 genome segment from
232 artiodactyl rotaviruses through intragenogroup reassortment as the closest related cognate VP3
233 encoding genome segments were those of bovine strain MPT-93 detected in Mozambique in
234 2015 and a caprine strain K-98 detected in India in 2015. They likely acquired their NSP2
235 genome segment from Wa-like rotaviruses intergenogroup reassortment as it was assigned an N1
236 genotype. Phylogenetically, the NSP2 for our reassortant strains was closely related to those that
237 were detected in the Czech Republic around 2019. We could not infer when and where exactly
238 the NSP2 reassortment events occurred due to the limited numbers of available rotavirus whole
239 genome sequence data from many countries. Similarly, the reassortant DS-1-like G3P[4] likely
240 acquired or donated their DS-1-like VP6, VP7, NSP1 and NSP4 from G3P[4] rotaviruses that
241 circulated in Islamabad and Rawalpindi in Pakistan from 2014-2016 (Umair et al. 2018; Sadiq et

242 al. 2019; Naqvi et al. 2020) As limited countries are conducting rotavirus genomic surveillance,
243 it is possible that these reassortment events occurred in an unsampled location prior to their
244 importation into Pakistan. Nevertheless, the resultant reassortant DS-1-like G3P[4] strains were
245 the ones that likely ended up in Malawi where they were associated with diarrhoea infections in
246 2017 and 2018 at QECH (Mhango et al. 2020) (Figure 5). Thus, the reassortant DS-1-like
247 G3P[4] strains were likely generated through a series of reassortment events elsewhere prior to
248 their circulation in Malawi.

249 Amino acid substitutions within antigenic regions of G3P[8] have potential 250 to drive vaccine escape variants

251 Antigenic regions of the rotavirus outer capsid proteins are critical for inducing neutralising
252 antibodies (Estes et al. 2007). We assessed if there were amino acid differences between
253 antigenic regions of the Malawian G3s strains to that of the G1P[8] Rotarix vaccine strain, and
254 determined the structural conformational differences resulting from these mismatches. Due to the
255 known amino acid mismatches between heterotypic rotavirus genotypes (Matthijnsens, Ciarlet,
256 Heiman, et al. 2008), this analysis was limited to homotypic genotypes hence only the VP4
257 proteins of the G3P[8] strains were compared to that of the G1P[8] Rotarix vaccine strain (P[8]
258 genotype). At least 32 out of the 36 amino acids that spans across the antigenic regions along the
259 VP5* and VP8* subunits of the VP4 for the G3P[8] strains matched those of the Rotarix strain
260 (Supplementary Table S3). The VP5* of the study G3P[8] strains (lineage III) were identical to
261 that of Rotarix strain (lineage I) across all antigenic regions (Supplementary Table S3).
262 However, differences were observed within the VP8*-1 and VP8*-3 antigenic regions. The
263 E150D was the only substitution along the VP8*-1 antigenic region, whereas S125N, S131R and
264 N135D substitutions occurred within the VP8*-3 antigenic region (Supplementary Table S4).
265 The S131R amino acid substitution within the VP8*-3 resulted in a change from a charged
266 amino acid with a potential of five hydrogen bonds to a polar amino acid with four hydrogen
267 bonds. When we aligned the VP8* protein structures of the G3P[8] study strains against that of
268 Rotarix strain, the superimposed structures revealed structural conformation differences within
269 antigenic epitope region 8*-1 and 8*-3 specifically at positions 150 as well as 131, respectively
270 (Supplementary Figure S4). The differences in the structural conformation of the antigenic

271 region has potential to impact the neutralising ability of the Rotarix vaccine-induced antibodies
272 against G3P[8] strains.

273 Discussion

274 In this study, we have shown that G3 rotaviruses that re-emerged in 2017 in Malawi, almost
275 twenty years after their last detection, became the predominant strains post-Rotarix vaccine
276 introduction after replacing G1 and G2 rotaviruses as typical human strains. This finding is
277 unique and in contrast with observations seen in most countries, including Australia, Italy,
278 Hungary, Spain, Japan and Kenya where the emergence of G3 strains has mostly been due to
279 equine-like G3 strains (Komoto et al. 2018; Dóro et al. 2016; Cowley et al. 2016; Luchs et al.
280 2019; Esposito et al. 2019; Mwanga et al. 2020). Through whole-genome sequencing, we
281 showed that the re-emergence of G3 strains in Malawi was not associated with a single genotype,
282 but rather four genotype variants; G3P[4] and G3P[6] with a DS-1-like constellation, G3P[8]
283 with a Wa-like constellation and G3P[4] genotypes with a DS-1-like backbone containing a
284 reassortant Wa-like NSP2 genome segment. Chronologically, these G3 rotaviruses circulated in
285 three phases in Malawi whereby the DS-1-like G3P[4] strains were the first to emerge in
286 November 2017 until August 2018 followed by a sporadic detection of DS-1-like G3P[6] in
287 September 2018, Wa-like G3P[8] from December 2018 to August 2019 and reassortant DS-1-
288 like G3P[4] from December 2018 until August 2019 with the Wa-like G3P[8] strains
289 predominating in the latter period (2018 to 2019). Phylogenetic analysis revealed that multiple
290 G3 lineages circulated in Malawi and that the re-emerging G3 strains did not arise due to
291 stepwise evolution of the previously circulating strains, but rather through genomic reassortment
292 and importation of strains from other countries. Altogether, these findings highlight the role of
293 genome reassortment in driving rotavirus evolution and human mobility in disseminating
294 rotavirus strains internationally.

295
296 Like other segmented viruses, such as influenza (Webster et al. 1992), rotaviruses frequently
297 reassort their genomic segments, which increases their genetic diversity (Martínez-Laso et al.
298 2009). Although the majority of the human-associated G3 strains have a P[8] and Wa-like
299 genotype constellation (Matthijnsens and Van Ranst 2012), most of the recently emerged G3
300 rotaviruses possess equine-like as well as DS-1-like rotavirus genome segments (Cowley et al.

301 2016; Dóró et al. 2016; Luchs et al. 2019; Komoto et al. 2018; Arana et al. 2016; Esposito et al.
302 2019). Whole genome sequencing of G3 rotavirus strains that were detected from other countries
303 has shown that intergenogroup reassortment events between human and equine rotaviruses drove
304 their emergence (Malasao et al. 2015). In contrast, the G3 strains that re-emerged in Malawi had
305 typical human Wa-like and DS-1-like genetic constellations. These findings were similar to
306 previous analysis of rotavirus genotypes that circulated in Malawi for over two decades from
307 1997 identified a diverse population of rotaviruses (at least 24 G and P genotype combinations)
308 of which WGS revealed the majority had either a Wa-like or DS-1-like genetic backbone
309 (Mhango et al. 2020; Jere et al. 2018). The four G3 variants that re-emerged in Malawi from
310 2017 also had either a Wa-like or DS-1-like genetic backbone but phylogenetic analysis revealed
311 up to four lineages in each genome segment (one in all Wa-like and up to three in DS-1-like).
312 This data demonstrates the wide diversity of G3 strains that co-circulated in Malawi within the
313 two-year study period.

314
315 Further phylogenetic analyses of the re-emergent G3P[4] strains revealed that two populations
316 circulated chronologically in Malawi. The DS-1-like G3P[4] strains that emerged first were
317 genetically closest to sequenced G3 strains from Asia (Pakistan), whereas the reassortant DS-1-
318 like G3P[4] strains, which emerged afterward were genetically distantly related to the former
319 DS-1-like G3P[4] strains in seven genome segments. Our phylogenetic analysis suggested that
320 the reassortant strains did not emerge from the DS-1-like G3P[4] that were first detected in
321 Malawi between 2017 and 2018. In addition, the two G3P[4] populations did not share a recent
322 common ancestor in NSP3, VP1, VP2 and VP4; thus, the reassortant DS-1-like strains were most
323 likely not progenies of the DS-1-like G3P[4] strains that re-emerged first in Malawi and may
324 have acquired these genome segments from elsewhere or could have been circulating
325 independently at very low frequencies in such a way that could not be picked by our surveillance
326 system. Indeed, three genome segments (NSP5, VP1 and VP4) of the reassortant DS-1-like
327 G3P[4] strains clustered closely with strains from Europe (Czech Republic) instead of other
328 contemporary DS-1-like G3 strains detected in Asia (Pakistan) or DS-1-like G3P[4] and non-G3
329 strains that circulated previously in Malawi. These findings suggested that these reassortant DS-
330 1-like G3P[4] strains were potentially imported from other countries, although we cannot
331 discount that these strains circulated previously in Malawi as we did not have sufficient

332 sequenced G3 strains before their disappearance in the 1990s. Similarly, phylogenetic analysis of
333 our reassortant DS-1-like G3P[4] showed that their Wa-like NSP2 (N1) genome segments were
334 genetically similar to those from Czech Republic than those from Malawi while the VP3 genome
335 segments showed a high nucleotide sequence similarity and clustered closely to Artiodactyl
336 rotavirus strains characterised elsewhere. Considering our genomic surveillance could not pick
337 up any of these animal-like genome segments, our findings suggested that the VP3 genome
338 segments were not acquired in Malawi; rather, the reassortant strains were potentially seeded into
339 Malawi already having this segment. Therefore, as none of the genome segments of the
340 reassortant DS-1-like G3P[4] resemble strains sequenced from Malawi at any time, it is likely
341 that the reassortant strains containing a Wa-like NSP2 acquired their VP7, VP6, NSP1 and NSP4
342 genome segments from G3P[4] through intragenogroup reassortment elsewhere prior to their
343 introduction into Malawi in 2018. Together, these findings suggest that the typical and
344 reassortant G3 strains that re-emerged in Malawi were potentially imported, suggesting that
345 importation of rotavirus strains may be an overlooked, but key driver for reseeding genotypes in
346 different countries (Mhango et al. 2020; Jere et al. 2018).

347
348 Emerging virus strains have been associated with mutations that render vaccines and other
349 therapies, such as monoclonal antibodies, less effective as seen with the severe acute respiratory
350 syndrome coronavirus 2 (SARS-CoV-2) (Starr et al. 2021). Previous studies have shown that the
351 VP5* and VP8* outer capsid proteins play a significant role in inducing neutralising antibodies
352 against rotaviruses (Ludert et al. 2002; Park et al. 2021; Ruggeri and Greenberg 1991; Zhao et
353 al. 2015). The VP5* protein of the Malawian G3P[8] strains were 100% conserved when
354 compared to that of Rotarix vaccine, consistent with previous studies that have reported that the
355 VP5* is a highly conserved protein (Rasebotsa et al. 2020; Mwangi et al. 2020). However, we
356 identified E150D nonsynonymous substitutions within the VP8*-1 antigenic region and S125N,
357 S131R and N135D substitutions within VP8*-3 antigenic region when we compared the VP4
358 (VP8*sub-unit) segments of our G3P[8] strains to that of the strain used in the Rotarix rotavirus
359 vaccine. These substitutions have been associated with lineage III strains that are currently
360 predominant in eastern and southern African countries where the Rotarix vaccine is used
361 (Rasebotsa et al. 2020; Mwangi et al. 2020; Maringa et al. 2021). We speculate that the structural
362 changes we observed in the VP8*-1 and VP8*-3 antigenic regions could reduce the binding of

363 the vaccine-induced antibodies thereby reducing the vaccine effectiveness. Further studies are
364 required to investigate the impact of these nonsynonymous amino acid changes to generate a
365 complete map of vaccine escape mutants and how they affect antibody neutralisation.

366
367 Our study has some limitations. Due to the destruction of the historical stool sample collected
368 through our rotavirus surveillance system as part of the polio containment campaign in Malawi,
369 we included only a few G3P[8] strains from the pre-rotavirus vaccine period sequenced earlier as
370 we were unable to sequence additional pre-vaccine strains. Therefore, although we have shown
371 that the re-emerged G3P[8] strains in Malawi are unlikely to have emerged from those
372 circulating in Malawi in the pre-vaccination era, we cannot completely rule out that these strains
373 did not emerge from other unsampled strains circulating during this period. We also understand
374 that the contextual rotavirus sequences obtained from GenBank are sparse as sequencing of
375 rotavirus strains is not routinely performed in many countries, which leads to massive
376 surveillance gaps globally. Because of this, we could only infer that the re-emerged G3 strains in
377 Malawi were imported but we cannot say with absolute certainty the country of origin for these
378 strains. In addition, we halted our rotavirus surveillance from 2020 to 2021 due to the COVID-19
379 pandemic, which prevented us from investigating G3 rotaviruses over a longer time period after
380 their re-emergence. Regardless, we were able to generate representative G3 strains across the
381 two years of rotavirus surveillance that covered the period when G3 genotypes were detected at
382 high frequency.

383
384 To our knowledge, our study provides the first comprehensive and systematic genomic
385 characterization of the re-emerging G3 rotavirus from Africa. Our findings demonstrates that
386 four G3 rotaviruses genotype variants resembling typical human rotaviruses re-emerged after
387 Rotarix rotavirus vaccine introduction twenty years after disappearing for almost twenty years in
388 Malawi, and their emergence appear to be likely driven by importation from other countries. Our
389 findings highlight the role of human mobility in driving the dissemination and temporal
390 dynamics of circulating rotaviruses internationally and demonstrates the importance of robust
391 rotavirus surveillance and whole genome sequencing to monitor strain dynamics to inform
392 infection prevention and control strategies in high disease burden settings.

393 Methods

394 Ethical approval

395 Informed consent was obtained from all the mothers or legal guardians for the children who were
396 involved in this study. This study was conducted according to the guidelines of the Declaration
397 of Helsinki and approved by the Research Ethics Committee of the University of Liverpool,
398 Liverpool, UK (000490) and the National Health Sciences Research Committee, Lilongwe,
399 Malawi (#867).

400 Sample collection, rotavirus genotyping and selection of rotavirus strains

401 Stool samples were collected from children <5 years old who presented with acute gastroenteritis
402 to the Queen Elizabeth Central Hospital (QECH) in Blantyre, Malawi through a rotavirus
403 surveillance platform which has been on-going since 1997 (Mhango et al. 2020). Acute
404 gastroenteritis was defined as the passage of at least 3 loose, or looser-than-normal stools every
405 24 hours for less than one week. Presence of rotaviruses in stool samples was confirmed using
406 Rotaclone[®] Enzyme Immunosorbent Assay (Rotaclone[®], Meridian Bioscience, Cincinnati, OH,
407 USA). The VP7 and VP4 genotypes for rotavirus positive samples were assigned using a
408 multiplex heminested reverse transcriptase polymerase chain reaction (RT-PCR) as described
409 previously (Mhango et al. 2020; Iturriza-Gomara et al. 1999). At least one specimen containing
410 rotavirus of G3 genotype was selected each calendar month from November 2017 to August
411 2019 for sequencing ($n=27$) (Supplementary Figure 1). Whole genomes for three G3 strains that
412 circulated between 1997 to 1999 collected and sequenced from our previous studies were also
413 analysed (Jere et al. 2018; Cunliffe et al. 2010).

414 Extraction of rotavirus double-stranded RNA and synthesis of 415 complementary DNA

416 Rotavirus dsRNA was extracted and purified as previously described (Jere et al. 2011, 2018). To
417 remove contaminating DNA, the extracted dsRNA was precipitated with lithium chloride
418 (Sigma-Aldrich, Dorset, UK) for 16 hrs at 4°C and treated with DNase I (Sigma-Aldrich, Dorset,
419 UK) as previously described (Jere et al. 2018). Purified dsRNA was quantified on Qubit 3.0
420 fluorometer (Life Technologies, CA, USA). A 1% 0.5 X Tris borate ethylenediaminetetraacetic

421 acid (TBE) agarose gel (Sigma-Aldrich, Dorset, UK) stained with SYBR green (Sigma-Aldrich,
422 Dorset, UK) electrophoresis was used to check the integrity of the extracted dsRNA and was
423 visualised on a BioDoc transilluminator. Complementary DNA (cDNA) was synthesised using
424 the Maxima H Minus Double-Stranded cDNA Synthesis Kit (Thermo Fisher Scientific,
425 Waltham, MA) and purification was done using the MSB[®] Spin PCRapace (Stratec) Purification
426 Kit as previously described (Mwangi et al. 2020; Rasebotsa et al. 2020).

427 DNA library preparation and whole genome sequencing

428 The Nextera XT DNA Library Preparation Kit (Illumina, San Diego, CA, USA) was used to
429 prepare DNA libraries following the manufacturer's instructions. Briefly, the Nextera[®]
430 transposome enzyme was used to target genomic DNA which was amplified using a limited
431 cycle PCR. AMPure XP magnetic beads (Beckman Coulter, Pasadena, CA, USA) and 80%
432 alcohol were used to clean-up the DNA libraries. Qubit 3.0 fluorometer (Invitrogen, Carlsbad,
433 CA, USA) was used to quantify the cleaned-up DNA libraries. The fragment size and quality of
434 libraries were assessed on Agilent 2100 BioAnalyzer[®] (Agilent Technologies, Waldbronn,
435 Germany). Paired end nucleotide sequences were then generated on a MiSeq[®] sequencer
436 (Illumina, San Diego, CA, USA) at the University of the Free State-Next Generation Sequencing
437 (UFS-NGS) Unit, Bloemfontein, South Africa as previously described (Mwangi et al. 2020;
438 Rasebotsa et al. 2020).

439 Sequence assembly and whole genome genotype determination

440 We checked the quality of the whole genome sequencing data using FASTQC (de Sena Brandine
441 and Smith 2019) and selected samples with quality score >30 for subsequent analysis. Illumina
442 adapter sequences were trimmed from the raw FASTQ sequence data using BBDuk trimmer
443 (version 2) (<https://sourceforge.net/projects/bbmap/>) embedded in Geneious Prime software
444 (version 2020.1.1) (Kearse and Sturrock, n.d.). Consensus sequences were generated through
445 mapping of trimmed Illumina reads to prototype rotavirus Wa-like (accession numbers
446 JX406747.1 - JX406757.1) and DS-1-like (accession numbers HQ650116.1 - HQ650126.1)
447 genogroup reference strains by Geneious Read Mapper (version 6.0.3) with the medium
448 sensitivity and iteratively fine-tuning parameters five times in Geneious Prime software (Kearse
449 and Sturrock, n.d.). The Geneious consensus tool was used to call the total quality consensus by

450 selecting a 60% highest quality threshold. The gene annotation and prediction tool in Geneious
451 Prime was used to annotate regions of low coverage (<200). To validate the consensus sequences
452 generated by mapping reads to reference sequences, we generated *de novo* assemblies using
453 Iterative Virus Assembler (IVA, version 1.0.3) pipeline (Hunt et al. 2015) for comparison. We
454 assigned the genotypes of each assembled genome segment using the Virus Resource Pathogen
455 (ViPR) online server for viral genotyping (Pickett et al. 2012).

456 Phylogenetic analysis

457 To compare our study strains to G3 rotaviruses characterised globally, we obtained the VP7
458 genome segment of G3 strains from the Virus Variation Resource in the GenBank (Hatcher et al.
459 2017). We selected genomic segments with a complete open reading frame (ORF) and aligned
460 them using MUSCLE (version 3.8.1551) (Edgar 2004). Maximum likelihood phylogenetic trees
461 were then generated in MEGAX (version 10.1.8) with generalised time reversible (GTR) and
462 Gamma heterogeneity DNA models. We performed 1000 bootstraps to assess the reliability of
463 the branching order and partitions in the phylogeny. Annotation of the phylogenetic trees was
464 done using Microreact online server (Argimón et al. 2016). To define lineages for VP7, VP4 and
465 DS-1-like genome segments (genotype 2), we used well-known lineage definition frameworks
466 based on Sadiq et al 2019, Rasebotsa et al 2020 and Agbemabiase et al. 2019 work, respectively.
467 Representative reference nucleotide sequences for DS-1-like genotypes for each genome
468 segment were obtained from the Virus Variation Resource in the GenBank database (Hatcher et
469 al. 2017). As there is no well-known lineage definition framework for Wa-like genome segments
470 (genotype 1), global as well as local genotype 1 sequences sampled across the pre-vaccine and
471 post-vaccine periods in Malawi were used as references. The nucleotide sequences for the ORFs
472 of our study strains and reference strains were multiple aligned using MUSCLE (version
473 3.8.1551) (Edgar 2004). Once aligned, the DNA test models in MEGAX (version 10.1.8)
474 (Tamura, Stecher, and Kumar 2021) were used to identify the optimal evolutionary model that
475 best fit the data for each segment. According to the corrected Akaike Information Criterion
476 (AIC’c) as previously described (Kumar et al. 2018), the GTR model with Gamma heterogeneity
477 across nucleotide sites was selected and 1000 bootstraps were used to assess the reliability of the
478 branching order and partitioning during the construction of maximum likelihood trees
479 (Felsenstein 1988).

480 Inference of the time to the most recent common ancestor

481 To estimate the most recent common ancestor (tMRCA) for each genome segment, we utilised
482 nucleotide sequences of all Wa-like and DS-1-like strains that circulated between 1997 to 2019
483 in Malawi. We did not do genome-specific analysis for the G3 and P[6] genotype of the VP7
484 and VP4, respectively, because we did not have sufficient sequences to conduct the analysis. The
485 reassortant Wa-like NSP2 (N1 genotype) genome segments for the double reassortant G3P[4]
486 study strains were analysed together with other Wa-like NSP2 genome segments. In brief, we
487 aligned genomic segments of previously circulating Wa-like and DS-1-like strains with the Wa-
488 like and DS-1-like G3 segments, respectively, using MAFFT (version 7.487) (Katoh and
489 Standley 2013). The alignments were trimmed at the 3' and 5' prime ends in order to generate
490 sequences of equal lengths while preserving the integrity of the ORF as a pre analytical process.
491 Trimmed alignments were then used to generate time-resolved trees using tree-time (version
492 0.8.0) (Sagulenko, Puller, and Neher 2018) and the trees were subsequently visualised and
493 annotated using Auspice (version 2.23.0) (Hadfield et al. 2018). We exported the time-resolved
494 trees from Auspice and visualised them using R (version 4.0.3). We used ladderized using the
495 'ladderize' function in ape (version 5.6.2) (Revell 2012) and rooted the tree based on an
496 outgroup sequence using the 'root' function implemented in phytools (version 0.7.70) (Revell
497 2012). We estimated the phylogenetic root-to tip distance based on the sum of branch lengths
498 (transformed to represent time in days) using 'distRoot' function in adephylo (version 1.1.11)
499 (Jombart, Balloux, and Dray 2010) and visualised the tree annotated with the genotypes for each
500 strain using the 'plot.phylo' function in the ape (version 5.6.2) package (Paradis and Schliep
501 2019).

502 Structure comparison between the outer capsid VP4 proteins of the G3P[8] 503 and Rotarix vaccine G1P[8] strains

504 To compare the antigenic sites of the VP4 of G3P[8] and that of Rotarix G1P[8] strains, we
505 aligned their VP4 amino acid sequences using MAFFT (version 7.487) (Katoh and Standley
506 2013). We targeted the VP5* and VP8* antigenic regions and extracted antigenic sites from the
507 alignments in MEGAX (version 10.1.8) (Tamura, Stecher, and Kumar 2021). To investigate the
508 impact of amino acid substitutions within the antigenic sites on the structural conformation of the
509 neutralising epitopes within the VP4 protein, we selected a representative VP4 amino acid

510 sequences for G3P[8] strains and conducted protein modelling using Modeller (version 9.25)
511 (Eswar et al. 2006). We selected three model structures with the highest Z-dope score and
512 conducted a structural assessment using SWISS-MODEL server. The protein structures were
513 visualised and annotated using PyMOL (version 2.4.1) (DeLano 2002).

514 Data Availability Statement

515 The clinical data presented in this study are available on request from the corresponding author.
516 The data are not publicly available due to ethical restrictions. The whole-genome sequencing
517 data generated for genome segments utilised in this project were submitted to the NCBI database
518 under accession numbers ON791851-792171.

519 Author Contributions

520 V.N.N., F.E.D, M.M.N., and K.C.J conceived, designed and sought funding for the study. M.I-
521 G., N.A.C., O.K., and K.C.J. collected clinical data and stool samples. C.M., J.J.M., E.C., P.M.
522 M.M.N., and K.C.J. performed the laboratory work. C.M., C.C., and K.C.J. carried out the
523 statistical and bioinformatics analysis. C.C., A.W.K., and K.C.J. supervised the study. C.M.,
524 C.C., and K.C.J. drafted the manuscript. M.M.N generated the whole genome sequence data.
525 C.M., A.B., E.C, J.J.M., O.K., C.M-B., K.G.B., B.K., K.C.J., C.M.D., M.D.E., A.D. S., P.M.
526 M.I-G, N.A.C., V.N.N., A.W.K., F.E.D., M.M.N, C.C., and K.C.J contributed to interpretation
527 of the data and writing the manuscript. All authors have read and approved the final manuscript.

528 Funding

529 This work was supported by research grants from the Wellcome Trust (Programme grant
530 number: 091909/Z/10/Z, Bill and Melinda Gates Foundation (grant number: OPP1180423), and
531 US Centers for Disease Control and Prevention (CDC) funds through World Health Organisation
532 (WHO) (grant number: 2018/815189-0). K.C.J. is a Wellcome International Training Fellow
533 supported by the Wellcome Trust (grant number: 201945/Z/16/Z). The funders had no role in the
534 study design, data collection and interpretation, or the decision to submit the work for
535 publication. The authors did not receive any financial support or other form of reward related to
536 the development of the manuscript. Therefore, findings and conclusions in this report are those

537 of the authors and do not necessarily represent the formal position of the funders. N.A.C., and
538 K.C.J are affiliated to the National Institute for Health Research (NIHR) Health Protection
539 Research Unit in Gastrointestinal Infections at the University of Liverpool, a partnership with the
540 UK Health Security Agency (UKHSA), in collaboration with University of Warwick. The views
541 expressed are those of the author(s) and not necessarily those of the NIHR, the Department of
542 Health and Social Care or UKHSA.

543 Acknowledgments

544 We acknowledge the support of the laboratory staff at the Malawi-Liverpool-Wellcome Trust
545 Clinical Research Programme, clinical research team and the study participants. We also
546 acknowledge the University of Free State Next Generation Sequencing (UFS-NGS) unit staff for
547 sequencing the G3 strains as part of the African Enterics Viral Genome Initiative (AEVGI).

548 Conflicts of Interest

549 M.I.-G. has received investigator-initiated research grant support from the GSK group of
550 companies and Sanofi Pasteur Merck Sharpe & Dohme and Merck. N.A.C. has received
551 investigator-initiated grant support for rotavirus research and honoraria for participation in
552 DSMB rotavirus vaccine meetings from the GSK group of companies and honoraria from Sanofi
553 Pasteur for rotavirus vaccine advisory board. K.C.J. has received investigator-initiated research
554 grant support from the GSK group of companies. C.M.D. has served on rotavirus advisory
555 boards for GSK; all payments were paid directly to an administrative fund held by Murdoch
556 Children's Research Institute.

557 References

- 558 Agbemabiase, Chantal Ama, Toyoko Nakagomi, Susan Afua Damanka, Francis Ekow Dennis,
559 Belinda Larteley Lartey, George Enyimah Armah, and Osamu Nakagomi. 2019. "Sub-
560 Genotype Phylogeny of the Non-G, Non-P Genes of Genotype 2 Rotavirus A Strains."
561 *PloS One* 14 (5): e0217422.
- 562 Arana, Ainara, Milagrosa Montes, Khuzwayo C. Jere, Miriam Alkorta, Miren Iturriza-Gómara,
563 and Gustavo Cilla. 2016. "Emergence and Spread of G3P[8] Rotaviruses Possessing an
564 Equine-like VP7 and a DS-1-like Genetic Backbone in the Basque Country (North of
565 Spain), 2015." *Infection, Genetics and Evolution: Journal of Molecular Epidemiology and
566 Evolutionary Genetics in Infectious Diseases* 44 (October): 137–44.
- 567 Argimón, Silvia, Khalil Abudahab, Richard J. E. Goater, Artemij Fedosejev, Jyothish Bhai,

- 568 Corinna Glasner, Edward J. Feil, et al. 2016. "Microreact: Visualizing and Sharing Data
569 for Genomic Epidemiology and Phylogeography." *Microbial Genomics* 2 (11): e000093.
- 570 Bányai, Krisztián, Brigitta László, Jazmin Duque, A. Duncan Steele, E. Anthony S. Nelson, Jon
571 R. Gentsch, and Umesh D. Parashar. 2012. "Systematic Review of Regional and
572 Temporal Trends in Global Rotavirus Strain Diversity in the Pre Rotavirus Vaccine Era:
573 Insights for Understanding the Impact of Rotavirus Vaccination Programs." *Vaccine* 30
574 Suppl 1 (April): A122-30.
- 575 Bar-Zeev, Naor, Khuzwayo C. Jere, Aisleen Bennett, Louisa Pollock, Jacqueline E. Tate,
576 Osamu Nakagomi, Miren Iturriza-Gomara, et al. 2016. "Population Impact and
577 Effectiveness of Monovalent Rotavirus Vaccination in Urban Malawian Children 3 Years
578 After Vaccine Introduction: Ecological and Case-Control Analyses." *Clinical Infectious
579 Diseases: An Official Publication of the Infectious Diseases Society of America* 62 Suppl
580 2 (May): S213-9.
- 581 Bennett, Aisleen, Louisa Pollock, Naor Bar-Zeev, Joseph A. Lewnard, Khuzwayo C. Jere,
582 Benjamin Lopman, Miren Iturriza-Gomara, Virginia E. Pitzer, and Nigel A. Cunliffe. 2021.
583 "Community Transmission of Rotavirus Infection in a Vaccinated Population in Blantyre,
584 Malawi: A Prospective Household Cohort Study." *The Lancet Infectious Diseases* 21 (5):
585 731–40.
- 586 Carvalho-Costa, Filipe A., Rosane M. S. de Assis, Alexandre M. Fialho, Irene T. Araújo,
587 Marcelle F. Silva, Mariela M. Gómez, Juliana S. Andrade, et al. 2019. "The Evolving
588 Epidemiology of Rotavirus A Infection in Brazil a Decade after the Introduction of
589 Universal Vaccination with Rotarix®." *BMC Pediatrics* 19 (1): 42.
- 590 Cates, Jordan E., Jacqueline E. Tate, and Umesh Parashar. 2022. "Rotavirus Vaccines:
591 Progress and New Developments." *Expert Opinion on Biological Therapy* 22 (3): 423–
592 32.
- 593 Chandran, Aruna, Sean Fitzwater, Anjie Zhen, and Mathuram Santosham. 2010. "Prevention of
594 Rotavirus Gastroenteritis in Infants and Children: Rotavirus Vaccine Safety, Efficacy,
595 and Potential Impact of Vaccines." *Biologics: Targets & Therapy* 4 (August): 213–29.
- 596 Clark, Andrew, Robert Black, Jacqueline Tate, Anna Roose, Karen Kotloff, Diana Lam, William
597 Blackwelder, et al. 2017. "Estimating Global, Regional and National Rotavirus Deaths in
598 Children Aged <5 Years: Current Approaches, New Analyses and Proposed
599 Improvements." *PloS One* 12 (9): e0183392.
- 600 Cowley, Daniel, Celeste M. Donato, Susie Roczo-Farkas, and Carl D. Kirkwood. 2016.
601 "Emergence of a Novel Equine-like G3P[8] Inter-Genogroup Reassortant Rotavirus
602 Strain Associated with Gastroenteritis in Australian Children." *The Journal of General
603 Virology* 97 (2): 403–10.
- 604 Cunliffe, Nigel A., Bagrey M. Ngwira, Winifred Dove, Benson D. M. Thindwa, Ann M. Turner,
605 Robin L. Broadhead, Malcolm E. Molyneux, and C. Anthony Hart. 2010. "Epidemiology
606 of Rotavirus Infection in Children in Blantyre, Malawi, 1997-2007." *The Journal of
607 Infectious Diseases* 202 Suppl (September): S168-74.
- 608 Degiuseppe, J. I., and J. A. Stupka. 2018. "First Assessment of All-Cause Acute Diarrhoea and
609 Rotavirus-Confirmed Cases Following Massive Vaccination in Argentina." *Epidemiology
610 and Infection* 146 (15): 1948–54.
- 611 DeLano, W. L. 2002. "Pymol: An Open-Source Molecular Graphics Tool." *CCP4 Newsl. Protein
612 Crystallogr.*
613 [http://citeseerx.ist.psu.edu/viewdoc/download?doi=10.1.1.231.5879&rep=rep1&type=pdf
614 #page=44.](http://citeseerx.ist.psu.edu/viewdoc/download?doi=10.1.1.231.5879&rep=rep1&type=pdf#page=44)
- 615 Donato, Celeste M., Susie Roczo-Farkas, Carl D. Kirkwood, Graeme L. Barnes, and Julie E.
616 Bines. 2022. "Rotavirus Disease and Genotype Diversity in Older Children and Adults in
617 Australia." *The Journal of Infectious Diseases* 225 (12): 2116–26.
- 618 Dóro, Renáta, Brigitta László, Vito Martella, Eyal Leshem, Jon Gentsch, Umesh Parashar, and

- 619 Krisztián Bányai. 2014. "Review of Global Rotavirus Strain Prevalence Data from Six
620 Years Post Vaccine Licensure Surveillance: Is There Evidence of Strain Selection from
621 Vaccine Pressure?" *Infection, Genetics and Evolution: Journal of Molecular
622 Epidemiology and Evolutionary Genetics in Infectious Diseases* 28 (December): 446–61.
- 623 Dóró, Renáta, Szilvia Marton, Anett Horváth Bartókné, György Lengyel, Zsófia Agócs, Ferenc
624 Jakab, and Krisztián Bányai. 2016. "Equine-like G3 Rotavirus in Hungary, 2015 - Is It a
625 Novel Intergenogroup Reassortant Pandemic Strain?" *Acta Microbiologica et
626 Immunologica Hungarica* 63 (2): 243–55.
- 627 Edgar, Robert C. 2004. "MUSCLE: Multiple Sequence Alignment with High Accuracy and High
628 Throughput." *Nucleic Acids Research* 32 (5): 1792–97.
- 629 Esposito, Susanna, Barbara Camilloni, Sonia Bianchini, Giovanni Ianiro, Ilaria Polinori, Edoardo
630 Farinelli, Marina Monini, and Nicola Principi. 2019. "First Detection of a Reassortant
631 G3P[8] Rotavirus A Strain in Italy: A Case Report in an 8-Year-Old Child." *Virology
632 Journal* 16 (1): 64.
- 633 Estes, M. K., A. Z. Kapikian, D. M. Knipe, and P. M. Howley. 2007. "Rotaviruses. Fields
634 Virology." *Eds) Knipe DM, Howley PM, Griffin DE, Lamb RA, Martin MA, Roizman B,
635 Straus SE, Philadelphia: Kluwer Health/Lippincott, Williams and Wilkins, 1917–74.*
- 636 Eswar, Narayanan, Ben Webb, Marc A. Marti-Renom, M. S. Madhusudhan, David Eramian,
637 Min-Yi Shen, Ursula Pieper, and Andrej Sali. 2006. "Comparative Protein Structure
638 Modeling Using Modeller." *Current Protocols in Bioinformatics / Editorial Board, Andreas
639 D. Baxevanis ... [et Al.] Chapter 5 (October): Unit-5.6.*
- 640 Felsenstein, J. 1988. "Phylogenies from Molecular Sequences: Inference and Reliability."
641 *Annual Review of Genetics* 22: 521–65.
- 642 Hadfield, James, Colin Megill, Sidney M. Bell, John Huddleston, Barney Potter, Charlton
643 Callender, Pavel Sagulenko, Trevor Bedford, and Richard A. Neher. 2018. "Nextstrain:
644 Real-Time Tracking of Pathogen Evolution." *Bioinformatics* 34 (23): 4121–23.
- 645 Hatcher, Eneida L., Sergey A. Zhdanov, Yiming Bao, Olga Blinkova, Eric P. Nawrocki, Yuri
646 Ostapchuck, Alejandro A. Schäffer, and J. Rodney Brister. 2017. "Virus Variation
647 Resource - Improved Response to Emergent Viral Outbreaks." *Nucleic Acids Research*
648 45 (D1): D482–90.
- 649 Henschke, N., H. Bergman, D. Hungerford, N. A. Cunliffe, R. F. Grais, G. Kang, U. D. Parashar,
650 S. A. Wang, and K. M. Neuzil. 2022. "The Efficacy and Safety of Rotavirus Vaccines in
651 Countries in Africa and Asia with High Child Mortality." *Vaccine* 40 (12): 1707–11.
- 652 Hungerford, Daniel, David J. Allen, Sameena Nawaz, Sarah Collins, Shamez Ladhani, Roberto
653 Vivancos, and Miren Iturriza-Gómara. 2019. "Impact of Rotavirus Vaccination on
654 Rotavirus Genotype Distribution and Diversity in England, September 2006 to August
655 2016." *Euro Surveillance: Bulletin European Sur Les Maladies Transmissibles =
656 European Communicable Disease Bulletin* 24 (6). [https://doi.org/10.2807/1560-
657 7917.ES.2019.24.6.1700774](https://doi.org/10.2807/1560-7917.ES.2019.24.6.1700774).
- 658 Hunt, Martin, Astrid Gall, Swee Hoe Ong, Jacqui Brener, Bridget Ferns, Philip Goulder, Eleni
659 Nastouli, Jacqueline A. Keane, Paul Kellam, and Thomas D. Otto. 2015. "IVA: Accurate
660 de Novo Assembly of RNA Virus Genomes." *Bioinformatics* 31 (14): 2374–76.
- 661 Iturriza-Gomara, M., J. Green, D. W. Brown, U. Desselberger, and J. J. Gray. 1999.
662 "Comparison of Specific and Random Priming in the Reverse Transcriptase Polymerase
663 Chain Reaction for Genotyping Group A Rotaviruses." *Journal of Virological Methods* 78
664 (1–2): 93–103.
- 665 Jere, Khuzwayo C., Chrispin Chaguza, Naor Bar-Zeev, Jenna Lowe, Chikondi Peno, Benjamin
666 Kumwenda, Osamu Nakagomi, et al. 2018. "Emergence of Double- and Triple-Gene
667 Reassortant G1P[8] Rotaviruses Possessing a DS-1-Like Backbone after Rotavirus
668 Vaccine Introduction in Malawi." *Journal of Virology* 92 (3).
669 <https://doi.org/10.1128/JVI.01246-17>.

- 670 Jere, Khuzwayo C., Luwanika Mlera, Hester G. O'Neill, A. Christiaan Potgieter, Nicola A. Page,
671 Mapaseka L. Seheri, and Alberdina A. van Dijk. 2011. "Whole Genome Analyses of
672 African G2, G8, G9, and G12 Rotavirus Strains Using Sequence-Independent
673 Amplification and 454® Pyrosequencing." *Journal of Medical Virology* 83 (11): 2018–42.
- 674 João, Eva D., Benilde Munlela, Assucênio Chissaque, Jorfélia Chilaúle, Jerónimo Langa,
675 Orvalho Augusto, Simone S. Boene, et al. 2020. "Molecular Epidemiology of Rotavirus A
676 Strains Pre- and Post-Vaccine (Rotarix®) Introduction in Mozambique, 2012-2019:
677 Emergence of Genotypes G3P[4] and G3P[8]." *Pathogens* 9 (9).
678 <https://doi.org/10.3390/pathogens9090671>.
- 679 Jombart, Thibaut, François Balloux, and Stéphane Dray. 2010. "Adephylo: New Tools for
680 Investigating the Phylogenetic Signal in Biological Traits." *Bioinformatics* 26 (15): 1907–
681 9.
- 682 Katoh, Kazutaka, and Daron M. Standley. 2013. "MAFFT Multiple Sequence Alignment
683 Software Version 7: Improvements in Performance and Usability." *Molecular Biology and
684 Evolution* 30 (4): 772–80.
- 685 Kearse, and Sturrock. n.d. "The Geneious 6.0. 3 Read Mapper." *Auckland University Law
686 Review*.
687 <http://assets.geneious.com.s3.amazonaws.com/documentation/geneious/GeneiousRead>
688 [Mapper.pdf](http://assets.geneious.com.s3.amazonaws.com/documentation/geneious/GeneiousRead).
- 689 Kirkwood, Carl D., and A. Duncan Steele. 2018. "Rotavirus Vaccines in China: Improvement Still
690 Required." *JAMA Network Open*.
- 691 Komoto, Satoshi, Tomihiko Ide, Manami Negoro, Takaaki Tanaka, Kazutoyo Asada, Masakazu
692 Umemoto, Haruo Kuroki, et al. 2018. "Characterization of Unusual DS-1-like G3P[8]
693 Rotavirus Strains in Children with Diarrhea in Japan." *Journal of Medical Virology* 90 (5):
694 890–98.
- 695 Kumar, Sudhir, Glen Stecher, Michael Li, Christina Knyaz, and Koichiro Tamura. 2018. "MEGA
696 X: Molecular Evolutionary Genetics Analysis across Computing Platforms." *Molecular
697 Biology and Evolution* 35 (6): 1547–49.
- 698 Luchs, Adriana, Antonio Charlys da Costa, Audrey Cilli, Shirley Cavalcante Vasconcelos
699 Komninakis, Rita de Cássia Compagnoli Carmona, Lais Boen, Simone Guadagnucci
700 Morillo, Ester Cerdeira Sabino, and Maria do Carmo Sampaio Tavares Timenetsky.
701 2019. "Spread of the Emerging Equine-like G3P[8] DS-1-like Genetic Backbone
702 Rotavirus Strain in Brazil and Identification of Potential Genetic Variants." *The Journal of
703 General Virology* 100 (1): 7–25.
- 704 Ludert, Juan Ernesto, Marie Christine Ruiz, Carlos Hidalgo, and Ferdinando Liprandi. 2002.
705 "Antibodies to Rotavirus Outer Capsid Glycoprotein VP7 Neutralize Infectivity by
706 Inhibiting Virion Decapsidation." *Journal of Virology* 76 (13): 6643–51.
- 707 Malasao, Rungnapa, Mayuko Saito, Akira Suzuki, Toshifumi Imagawa, Nao Nukiwa-Soma,
708 Kentaro Tohma, Xiaofang Liu, et al. 2015. "Human G3P[4] Rotavirus Obtained in Japan,
709 2013, Possibly Emerged through a Human-Equine Rotavirus Reassortment Event."
710 *Virus Genes* 50 (1): 129–33.
- 711 Maringa, Wairimu M., Julia Simwaka, Peter N. Mwangi, Evans M. Mpabalwani, Jason M.
712 Mwenda, M. Jeffrey Mphahlele, Mapaseka L. Seheri, and Martin M. Nyaga. 2021.
713 "Whole Genome Analysis of Human Rotaviruses Reveals Single Gene Reassortant
714 Rotavirus Strains in Zambia." *Viruses* 13 (9). <https://doi.org/10.3390/v13091872>.
- 715 Martínez-Laso, Jorge, Angela Román, Miriam Rodríguez, Isabel Cervera, Jacqueline Head, Iciar
716 Rodríguez-Avial, and Juan J. Picazo. 2009. "Diversity of the G3 Genes of Human
717 Rotaviruses in Isolates from Spain from 2004 to 2006: Cross-Species Transmission and
718 Inter-Genotype Recombination Generates Alleles." *The Journal of General Virology* 90
719 (Pt 4): 935–43.
- 720 Matthijnssens, Jelle, Max Ciarlet, Erica Heiman, Ingrid Arijs, Thomas Delbeke, Sarah M.

- 721 McDonald, Enzo A. Palombo, et al. 2008. "Full Genome-Based Classification of
722 Rotaviruses Reveals a Common Origin between Human Wa-Like and Porcine Rotavirus
723 Strains and Human DS-1-like and Bovine Rotavirus Strains." *Journal of Virology* 82 (7):
724 3204–19.
- 725 Matthijnssens, Jelle, Max Ciarlet, Mustafizur Rahman, Houssam Attoui, Krisztián Bányai, Mary
726 K. Estes, Jon R. Gentsch, et al. 2008. "Recommendations for the Classification of Group
727 A Rotaviruses Using All 11 Genomic RNA Segments." *Archives of Virology* 153 (8):
728 1621–29.
- 729 Matthijnssens, Jelle, Mustafizur Rahman, Vito Martella, Yang Xuelei, Sofie De Vos, Karolien De
730 Leener, Max Ciarlet, Canio Buonavoglia, and Marc Van Ranst. 2006. "Full Genomic
731 Analysis of Human Rotavirus Strain B4106 and Lapine Rotavirus Strain 30/96 Provides
732 Evidence for Interspecies Transmission." *Journal of Virology* 80 (8): 3801–10.
- 733 Matthijnssens, Jelle, and Marc Van Ranst. 2012. "Genotype Constellation and Evolution of
734 Group A Rotaviruses Infecting Humans." *Current Opinion in Virology* 2 (4): 426–33.
- 735 Mhango, Chimwemwe, Jonathan J. Mandolo, End Chinyama, Richard Wachepa, Oscar
736 Kanjerwa, Chikondi Malamba-Banda, Prisca B. Matambo, et al. 2020. "Rotavirus
737 Genotypes in Hospitalized Children with Acute Gastroenteritis Before and After
738 Rotavirus Vaccine Introduction in Blantyre, Malawi, 1997 - 2019." *The Journal of
739 Infectious Diseases*, October. <https://doi.org/10.1093/infdis/jiaa616>.
- 740 Mwanga, Mike J., Jennifer R. Verani, Richard Omore, Jacqueline E. Tate, Umesh D. Parashar,
741 Nickson Murunga, Elijah Gicheru, Robert F. Breiman, D. James Nokes, and Charles N.
742 Agoti. 2020. "Multiple Introductions and Predominance of Rotavirus Group A Genotype
743 G3P[8] in Kilifi, Coastal Kenya, 4 Years after Nationwide Vaccine Introduction."
744 *Pathogens* 9 (12). <https://doi.org/10.3390/pathogens9120981>.
- 745 Mwangi, Peter N., Milton T. Mogotsi, Mapaseka L. Seheri, M. Jeffrey Mphahlele, Ina Peenze,
746 Mathew D. Esona, Benjamin Kumwenda, et al. 2020. "Whole Genome In-Silico Analysis
747 of South African G1P[8] Rotavirus Strains Before and After Vaccine Introduction Over A
748 Period of 14 Years." *Vaccines* 8 (4). <https://doi.org/10.3390/vaccines8040609>.
- 749 Naqvi, Syeda Sumera, Sundus Javed, Saadia Naseem, Asma Sadiq, Netasha Khan, Sadia
750 Sattar, Naseer Ali Shah, and Nazish Bostan. 2020. "G3 and G9 Rotavirus Genotypes in
751 Waste Water Circulation from Two Major Metropolitan Cities of Pakistan." *Scientific
752 Reports* 10 (1): 8665.
- 753 Paradis, Emmanuel, and Klaus Schliep. 2019. "Ape 5.0: An Environment for Modern
754 Phylogenetics and Evolutionary Analyses in R." *Bioinformatics* 35 (3): 526–28.
- 755 Park, Wook-Jin, Yeon-Kyung Yoon, Ji-Sun Park, Ruchirkumar Pansuriya, Yeong-Jae Seok, and
756 Ravi Ganapathy. 2021. "Rotavirus Spike Protein Δ Vp8* as a Novel Carrier Protein for
757 Conjugate Vaccine Platform with Demonstrated Antigenic Potential for Use as Bivalent
758 Vaccine." *Scientific Reports* 11 (1): 22037.
- 759 Pickett, Brett E., Douglas S. Greer, Yun Zhang, Lucy Stewart, Liwei Zhou, Guangyu Sun,
760 Zhiping Gu, et al. 2012. "Virus Pathogen Database and Analysis Resource (ViPR): A
761 Comprehensive Bioinformatics Database and Analysis Resource for the Coronavirus
762 Research Community." *Viruses* 4 (11): 3209–26.
- 763 Rasebotsa, Sebotsana, Peter N. Mwangi, Milton T. Mogotsi, Saheed Sabiu, Nonkululeko B.
764 Magagula, Kebareng Rakau, Jeannine Uwimana, et al. 2020. "Whole Genome and In-
765 Silico Analyses of G1P[8] Rotavirus Strains from Pre- and Post-Vaccination Periods in
766 Rwanda." *Scientific Reports* 10 (1): 13460.
- 767 Revell, Liam J. 2012. "Phytools: An R Package for Phylogenetic Comparative Biology (and
768 Other Things)." *Methods in Ecology and Evolution*. [https://doi.org/10.1111/j.2041-
769 210x.2011.00169.x](https://doi.org/10.1111/j.2041-210x.2011.00169.x).
- 770 Roczo-Farkas, Susie, Carl D. Kirkwood, Daniel Cowley, Graeme L. Barnes, Ruth F. Bishop,
771 Nada Bogdanovic-Sakran, Karen Boniface, Celeste M. Donato, and Julie E. Bines. 2018.

- 772 “The Impact of Rotavirus Vaccines on Genotype Diversity: A Comprehensive Analysis of
773 2 Decades of Australian Surveillance Data.” *The Journal of Infectious Diseases* 218 (4):
774 546–54.
- 775 Ruggeri, F. M., and H. B. Greenberg. 1991. “Antibodies to the Trypsin Cleavage Peptide VP8
776 Neutralize Rotavirus by Inhibiting Binding of Virions to Target Cells in Culture.” *Journal*
777 *of Virology* 65 (5): 2211–19.
- 778 Sadiq, Asma, Nazish Bostan, Habib Bokhari, Kwe Claude Yinda, and Jelle Matthijnsens. 2019.
779 “Whole Genome Analysis of Selected Human Group A Rotavirus Strains Revealed
780 Evolution of DS-1-Like Single- and Double-Gene Reassortant Rotavirus Strains in
781 Pakistan During 2015-2016.” *Frontiers in Microbiology* 10 (November): 2641.
- 782 Sagulenko, Pavel, Vadim Puller, and Richard A. Neher. 2018. “TreeTime: Maximum-Likelihood
783 Phylodynamic Analysis.” *Virus Evolution* 4 (1): vex042.
- 784 Saha, Debasish, Martin O. C. Ota, Priya Pereira, Philippe Buchy, and Selim Badur. 2021.
785 “Rotavirus Vaccines Performance: Dynamic Interdependence of Host, Pathogen and
786 Environment.” *Expert Review of Vaccines* 20 (8): 945–57.
- 787 Sena Brandine, Guilherme de, and Andrew D. Smith. 2019. “Falco: High-Speed FastQC
788 Emulation for Quality Control of Sequencing Data.” *F1000Research* 8 (November):
789 1874.
- 790 Starr, Tyler N., Allison J. Greaney, Adam S. Dingens, and Jesse D. Bloom. 2021. “Complete
791 Map of SARS-CoV-2 RBD Mutations That Escape the Monoclonal Antibody LY-CoV555
792 and Its Cocktail with LY-CoV016.” *BioRxiv : The Preprint Server for Biology*, February.
793 <https://doi.org/10.1101/2021.02.17.431683>.
- 794 Tamura, Koichiro, Glen Stecher, and Sudhir Kumar. 2021. “MEGA11: Molecular Evolutionary
795 Genetics Analysis Version 11.” *Molecular Biology and Evolution* 38 (7): 3022–27.
- 796 Troeger, Christopher, Ibrahim A. Khalil, Puja C. Rao, Shujin Cao, Brigette F. Blacker, Tahmeed
797 Ahmed, George Armah, et al. 2018. “Rotavirus Vaccination and the Global Burden of
798 Rotavirus Diarrhea Among Children Younger Than 5 Years.” *JAMA Pediatrics* 172 (10):
799 958–65.
- 800 Umair, Massab, Bilal Haider Abbasi, Salmaan Sharif, Muhammad Masroor Alam, Muhammad
801 Suleman Rana, Ghulam Mujtaba, Yasir Arshad, M. Qaiser Fatmi, and Sohail Zahoor
802 Zaidi. 2018. “High Prevalence of G3 Rotavirus in Hospitalized Children in Rawalpindi,
803 Pakistan during 2014.” *PloS One* 13 (4): e0195947.
- 804 “VIEW-Hub by IVAC.” n.d. VIEW-Hub by IVAC. Accessed September 23, 2022. [https://view-](https://view-hub.org/map/?set=current-vaccine-intro-status&group=vaccine-introduction&category=rv)
805 [hub.org/map/?set=current-vaccine-intro-status&group=vaccine-](https://view-hub.org/map/?set=current-vaccine-intro-status&group=vaccine-introduction&category=rv)
806 [introduction&category=rv](https://view-hub.org/map/?set=current-vaccine-intro-status&group=vaccine-introduction&category=rv).
- 807 Vizzi, Esmeralda, Oscar A. Piñeros, M. Daniela Oropeza, Laura Naranjo, José A. Suárez, Rixio
808 Fernández, José L. Zambrano, Argelia Celis, and Ferdinando Liprandi. 2017. “Human
809 Rotavirus Strains Circulating in Venezuela after Vaccine Introduction: Predominance of
810 G2P[4] and Reemergence of G1P[8].” *Virology Journal* 14 (1): 58.
- 811 Wahyuni, Rury Mega, Takako Utsumi, Zayyin Dinana, Laura Navika Yamani, Juniastuti, Ishak
812 Samuel Wuwuti, Elsa Fitriana, et al. 2021. “Prevalence and Distribution of Rotavirus
813 Genotypes Among Children With Acute Gastroenteritis in Areas Other Than Java Island,
814 Indonesia, 2016-2018.” *Frontiers in Microbiology* 12 (May): 672837.
- 815 Webster, R. G., W. J. Bean, O. T. Gorman, T. M. Chambers, and Y. Kawaoka. 1992. “Evolution
816 and Ecology of Influenza A Viruses.” *Microbiological Reviews* 56 (1): 152–79.
- 817 Zhao, Bingxin, Xiaoxia Pan, Yumei Teng, Wen Yue Xia, Jing Wang, Yuling Wen, and Yuanding
818 Chen. 2015. “Rotavirus VP7 Epitope Chimeric Proteins Elicit Cross-Immunoreactivity in
819 Guinea Pigs.” *Virologica Sinica* 30 (5): 363–70.
- 820
821

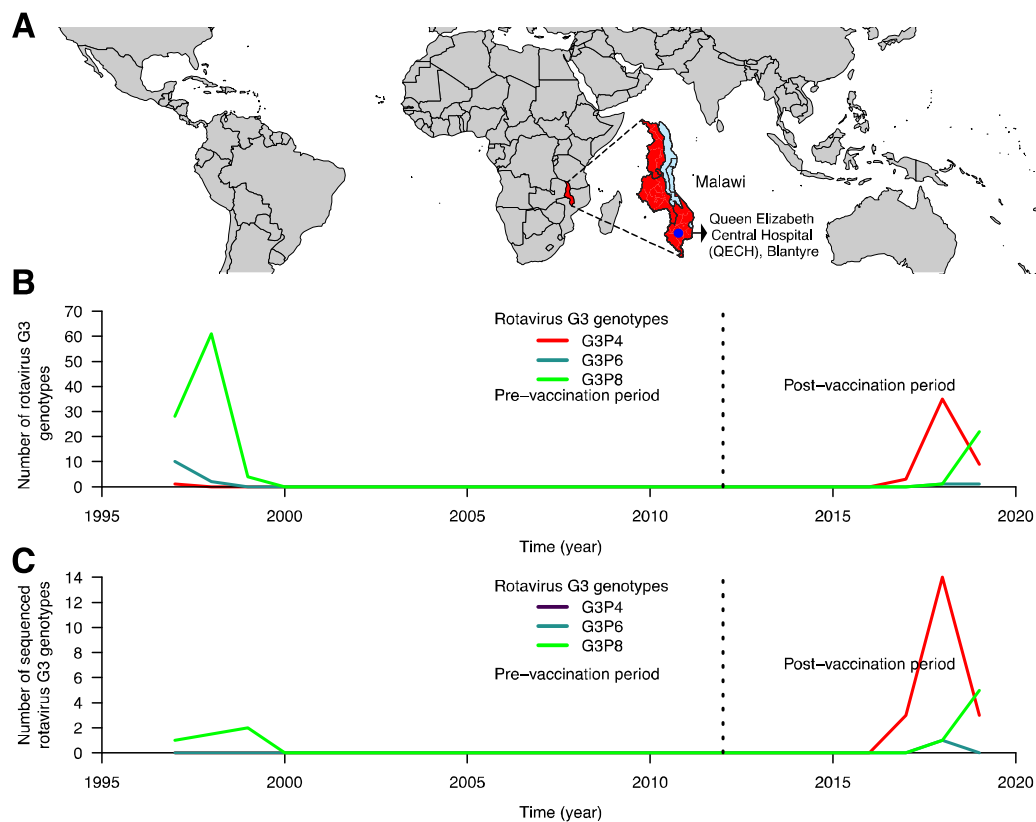


Figure 1. Rotavirus G3 genotypes and whole genome sequences characterised at Queen Elizabeth Central Hospital, Malawi before and after rotavirus vaccine introduction. (A) Global map highlighting the geographical location of Malawi in Africa as well as the location of Queen Elizabeth Central Hospital (QECH) in Malawi where the diarrhoea surveillance platform is set up. **(B)** Absolute number of PCR positive G3 rotavirus strains genotyped before and after Rotarix rotavirus vaccine introduction at QECH. **(C)** Absolute number of G3 whole genome sequences generated from stool specimens collected before and after Rotarix rotavirus vaccine introduction in Malawi.

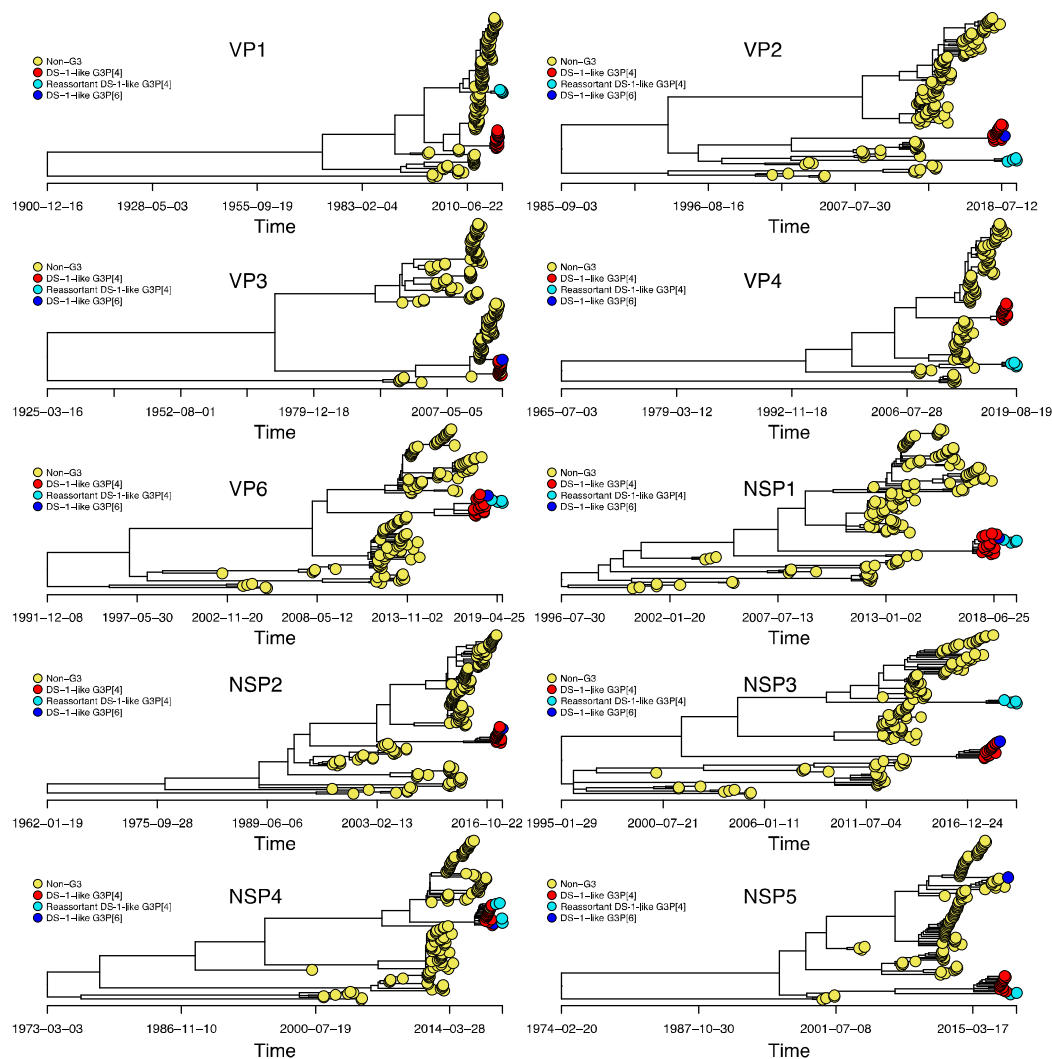


Figure 2. Time resolved phylogenetic trees for DS-1-like genome segments associated with G3 as well as non-G3 rotavirus strains detected in Malawi from 1997 to 2019. Only previously circulating DS-1-like genome segments with a complete open reading frame were used to estimate the time to the most common recent ancestor for the DS-1-like (G3P[4], G3P[6] and reassortant G3P[4]) in relation to locally circulating strains. Time trees were constructed using Nextstrain. The VP4 tree only contains genotype P[4]. The tips of DS-1-like G3P[4], DS-1-like G3P[6] and reassortant DS-1-like G3P[4] segments are annotated in red, blue and light blue colours respectively while all non-G3 genome segments are annotated in yellow colours.

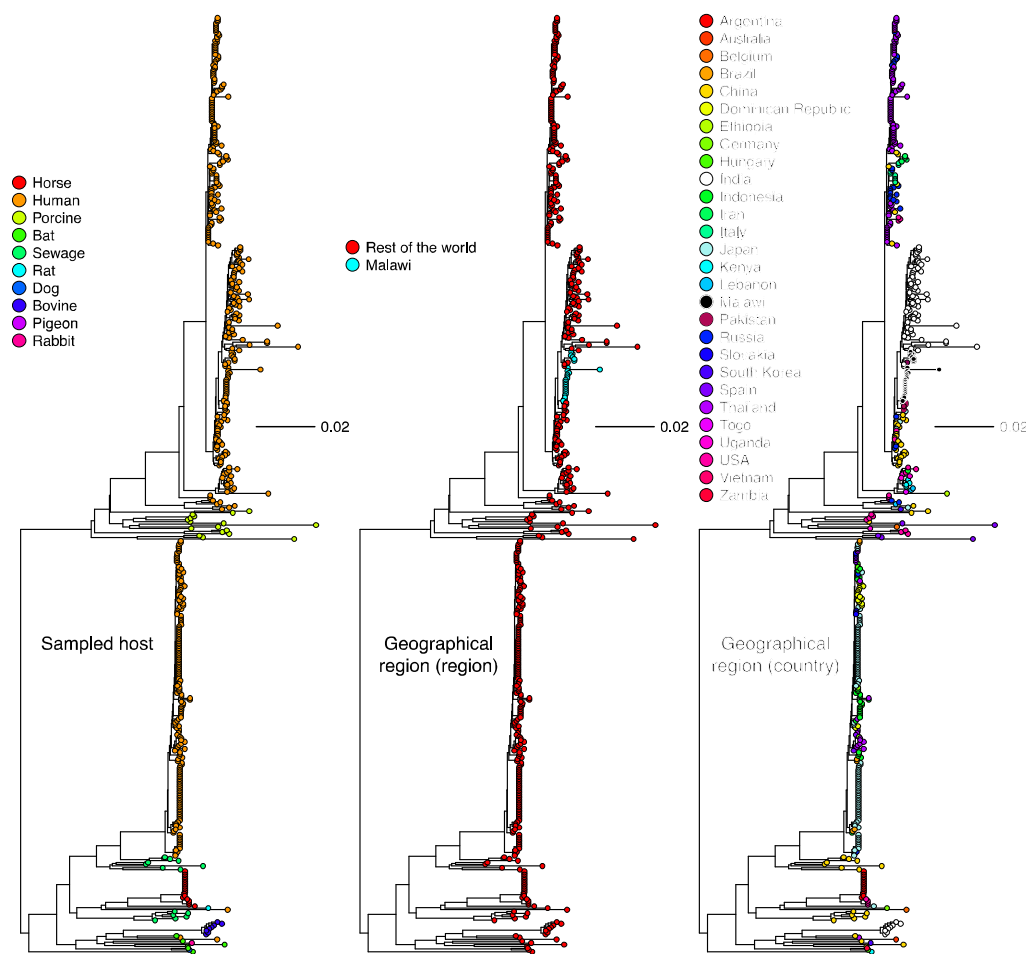


Figure 3. Global Maximum Likelihood phylogenetic trees for VP7 genome segments encoding the genotype G3. Only genome segments with a complete open reading frame characterised between 2010 to 2019 were included in the analysis. The GTR evolutionary model with Gamma heterogeneity across nucleotide sites was used for phylogenetic inference while 1000 bootstraps were used to assess the reliability of the branching order. The tree was rooted using the RVA/Pigeon-wt/JPN/PO-13/1989/G18P[17] but the outgroups were omitted for better visualisation.

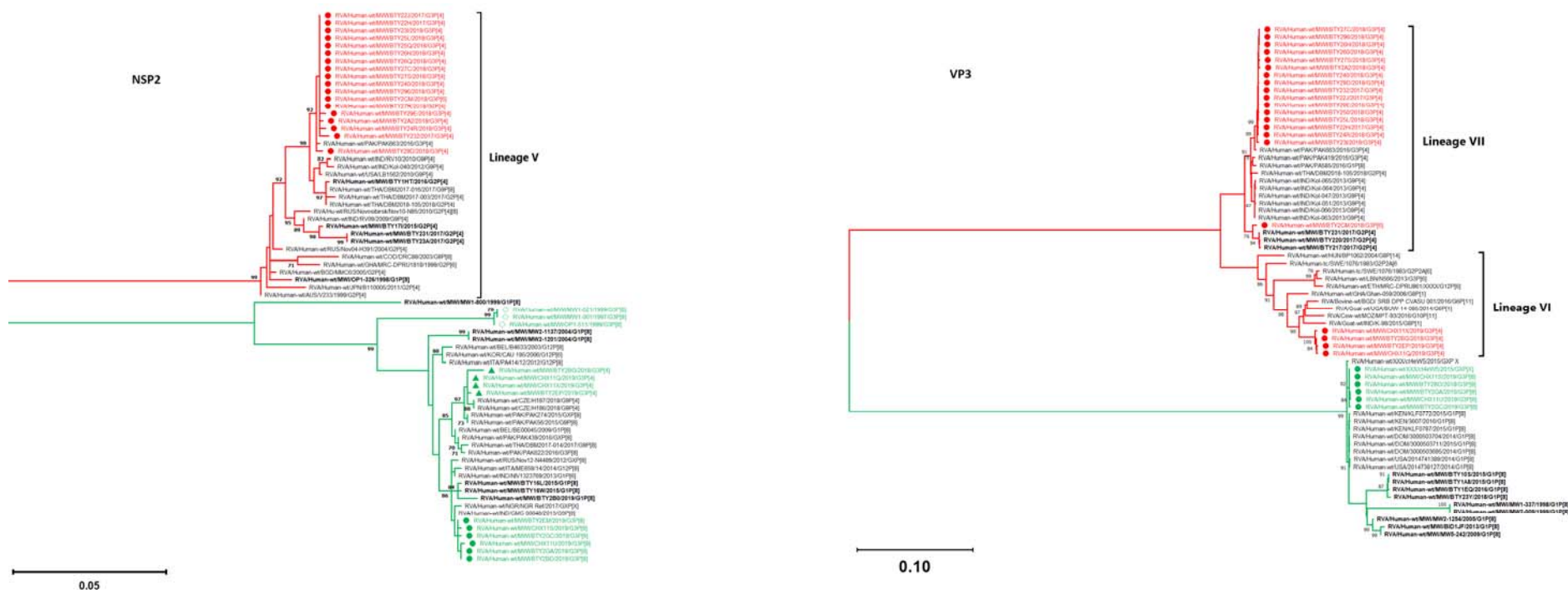


Figure 4. Maximum likelihood (ML) phylogenetic trees based on complete open reading frame of rotavirus NSP2 and VP3 genome segments. The trees were out grouped at RVA/Pigeon-wt/JPN/PO-13/1983/G18P[17] but were omitted for clear visualisation. The GTR evolutionary model with Gamma heterogeneity across nucleotide sites was used for phylogenetic inference. Bootstrap values $\geq 70\%$ are shown adjacent to each branch node. Genotype 1 (Wa-like) and 2 (DS-1-like) branches are annotated in green and red respectively. The strain names of Malawian Wa-like and DS-1-like G3 genome segments are denoted by green and red colours respectively. Circles represent post-vaccine while diamonds represent pre-vaccine Malawian G3 strains. Reassortant G3P[4] are represented by green triangles in (NSP2).

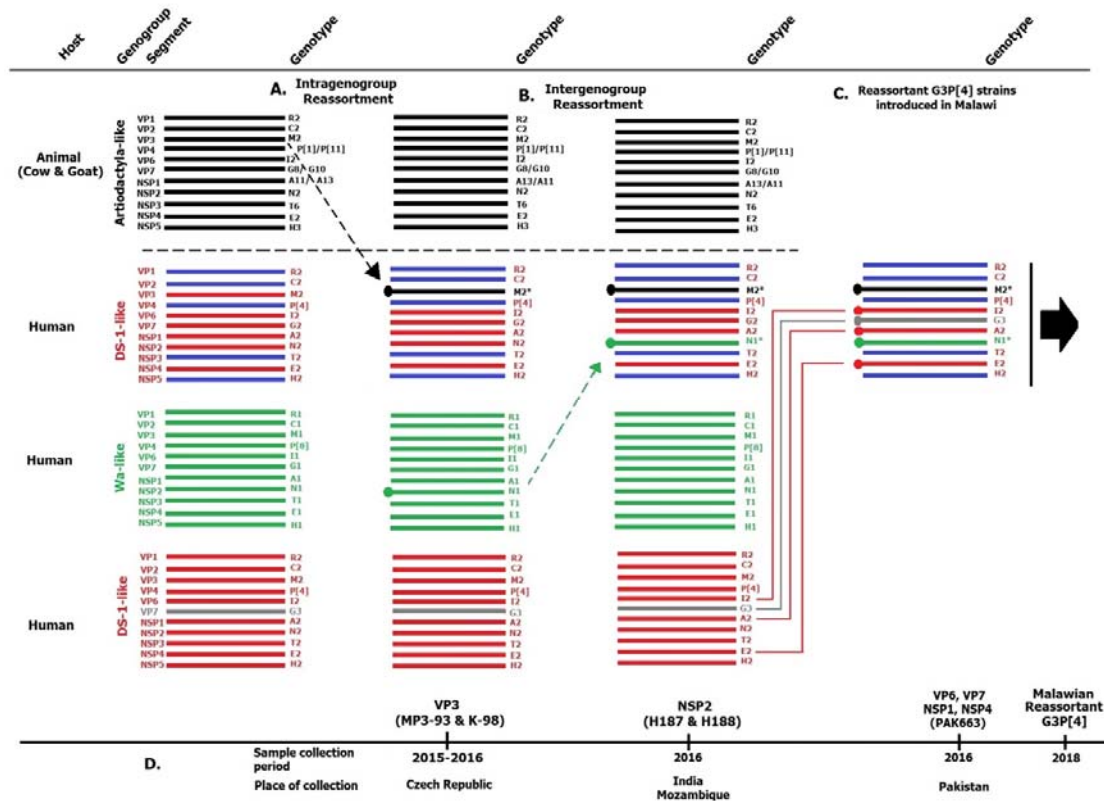


Figure 5. Reconstruction of the sequence of reassortment events that potentially lead to the emergence of the reassortant G3P[4] strains that were detected in Malawi. The reassortment events were hypothesised based on the genetic relationships between the genome segments of the reassortant DS-1-like G3P[4] rotaviruses that were detected in Malawi and those available in the NCBI Genbank to date. (A) The reassortant DS-1-like G3P[4] rotavirus strains that were detected in Malawi likely acquired their VP1, VP2, VP4, NSP1 and NSP5 genome segments from human DS-1-like rotaviruses and their VP3 from artiodactyl rotaviruses that circulated in countries where circulating rotaviruses have not been sequenced yet, or if done, their full-length genome sequences have not yet been deposited to the NCBI Genbank. (B) Both inter genogroup and intragenogroup reassortment events between Wa and DS-1-like rotaviruses were likely taking place from these unsampled regions, of which various progeny rotavirus populations were possibly generated. Reassortant DS-1-like strains that acquired their NSP2 through intergenogroup reassortment from Wa-like strains, which shared closest nucleotide similarity with rotaviruses that circulated in countries like Czech Republic between 2015 and 2016. (C) Various evolutionary events likely took place between the reassortant DS-1-like rotaviruses, DS-1-like G3P[4] and Wa-like G3P[8] rotaviruses that circulated in regions like Pakistan between 2014 – 2016, and in other unsampled regions that potentially led to various progeny rotavirus populations. One of the resultant progeny populations could be the reassortant DS-1-like G3P[4] strains from (B) that acquired NSP1, NSP4, VP6 and VP7 from the DS-1-like G3P[4] strains that were circulating in regions like Pakistan through complex reassortment events. The resultant reassortant DS-1-like G3P[4] rotaviruses were the ones that were exported to Malawi and caused diarrhoea disease in children that were hospitalised at Queen Elizabeth Central Hospital in Blantyre, Malawi from 2018, or circulated in unsampled regions. (D) The period and country where the closest related strains to the genome segments of the reassortant DS-1-like G3P[4] were detected. The horizontal line represents the 11 rotavirus genome segments.

The colours represent the following: Green - Wa-like genome segments; Red - DS-1-like genome segments; Black - Artiodactyla-like genome segments; Grey - G3 genotype; Blue - Distinct genome segments.

Table 1. Whole genotype constellations of pre- and post-vaccine Malawian G3 strains. The nomenclature of all the rotavirus strains indicates the rotavirus group, species where the strain was isolated, name of the country where the strain was originally isolated, the common name, year of isolation and the genotypes for genome segment 4 and 9 as proposed by the *Rotavirus Classification Working Group* (RCWG) (Matthijssens et al. 2008).

Strain Nomenclature	Genotype constellation											Genogroup/ Constellation	
	VP7	VP4	VP6	VP1	VP2	VP3	NSP1	NSP2	NSP3	NSP4	NSP5		
Pre-vaccine strains													
RVA/Human-wt/MWI/MW1-001/1997/G3P[8]	G3	P[8]	I1	R1	C1	M1	A1	N1	T1	E1	H1	Wa-like	
RVA/Human-wt/MWI/MW1-621/1999/G3P[8]	G3	P[8]	I1	R1	C1	M1	A1	N1	T1	E1	H1	Wa-like	
RVA/Human-wt/MWI/OP1-511/1999/G3P[8]	G3	P[8]	I1	R1	C1	M1	A1	N1	T1	E1	H1	Wa-like	
Post-vaccine strains													
RVA/Human-wt/MWI/BTY22H/2017/G3P[4]	G3	P[4]	I2	R2	C2	M2	A2	N2	T2	-	H2	DS-1-like	
RVA/Human-wt/MWI/BTY22J/2017/G3P[4]	G3	P[4]	I2	R2	C2	M2	A2	N2	T2	E2	H2	DS-1-like	
RVA/Human-wt/MWI/BTY232/2017/G3P[4]	G3	P[4]	I2	R2	C2	M2	A2	N2	T2	E2	H2	DS-1-like	
RVA/Human-wt/MWI/BTY23I/2018/G3P[4]	G3	P[4]	I2	R2	C2	M2	A2	N2	T2	E2	-	DS-1-like	
RVA/Human-wt/MWI/BTY240/2018/G3P[4]	G3	P[4]	I2	R2	C2	M2	A2	N2	T2	E2	H2	DS-1-like	
RVA/Human-wt/MWI/BTY24R/2018/G3P[4]	G3	P[4]	I2	R2	C2	M2	A2	N2	T2	E2	H2	DS-1-like	
RVA/Human-wt/MWI/BTY25Q/2018/G3P[4]	G3	P[4]	I2	R2	C2	M2	A2	N2	T2	E2	H2	DS-1-like	
RVA/Human-wt/MWI/BTY25L/2018/G3P[4]	G3	P[4]	I2	R2	C2	M2	A2	N2	T2	E2	H2	DS-1-like	

RVA/Human-wt/MWI/BTY26Q/2018/G3P[4]	G3	P[4]	I2	R2	C2	M2	A2	N2	T2	E2	H2	DS-1-like
RVA/Human-wt/MWI/BTY26H/2018/G3P[4]	G3	P[4]	I2	R2	C2	M2	A2	N2	T2	E2	H2	DS-1-like
RVA/Human-wt/MWI/BTY27C/2018/G3P[4]	G3	P[4]	I2	R2	C2	M2	A2	N2	T2	E2	H2	DS-1-like
RVA/Human-wt/MWI/BTY27S/2018/G3P[4]	G3	P[4]	I2	R2	C2	M2	A2	N2	T2	E2	H2	DS-1-like
RVA/Human-wt/MWI/BTY296/2018/G3P[4]	G3	P[4]	I2	R2	C2	M2	A2	N2	T2	E2	H2	DS-1-like
RVA/Human-wt/MWI/BTY29D/2018/G3P[4]	G3	P[4]	I2	R2	C2	M2	A2	N2	T2	E2	H2	DS-1-like
RVA/Human-wt/MWI/BTY29E/2018/G3P[4]	G3	P[4]	I2	R2	C2	M2	A2	N2	T2	E2	-	DS-1-like
RVA/Human-wt/MWI/BTY2A2/2018/G3P[4]	G3	-	I2	R2	C2	M2	A2	N2	T2	E2	-	DS-1-like
RVA/Human-wt/MWI/BTY2CM/2018/G3P[6]	G3	P[6]	I2	R2	C2	M2	A2	N2	T2	E2	H2	DS-1-like
RVA/Human-wt/MWI/BTY2BG/2018/G3P[4]	G3	P[4]	I2	R2	C2	M2	A2	N1	T2	E2	H2	Reassortant
RVA/Human-wt/MWI/BTY2EP/2019/G3P[4]	G3	P[4]	I2	R2	C2	M2	A2	N1	T2	E2	-	Reassortant
RVA/Human-wt/MWI/CHX11Q/2019/G3P[4]	G3	P[4]	I2	R2	C2	M2	A2	N1	T2	E2	H2	Reassortant
RVA/Human-wt/MWI/CHX11X/2019/G3P[4]	G3	P[4]	I2	R2	C2	M2	A2	N1	T2	E2	-	Reassortant
RVA/Human-wt/MWI/BTY2BD/2018/G3P[8]	G3	P[8]	I1	R1	C1	M1	A1	N1	T1	E1	H1	Wa-like

RVA/Human-wt/MWI/BTY2EM/2019/G3P[8]	G3	P[8]	I1	R1	C1	M1	A1	N1	T1	E1	H1	Wa-like
RVA/Human-wt/MWI/BTY2GA/2019/G3P[8]	G3	P[8]	I1	R1	C1	M1	A1	N1	T1	E1	H1	Wa-like
RVA/Human-wt/MWI/BTY2GC/2019/G3P[8]	G3	P[8]	I1	R1	C1	M1	A1	N1	T1	E1	H1	Wa-like
RVA/Human-wt/MWI/CHX11U/2019/G3P[8]	G3	P[8]	I1	R1	C1	M1	A1	N1	T1	E1	H1	Wa-like
RVA/Human-wt/MWI/CHX11S/2019/G3P[8]	G3	P[8]	I1	R1	C1	M1	A1	N1	T1	E1	H1	Wa-like

Table 2. Time to the most recent common ancestor (tMRCA) for Malawian Wa-like and DS-1-like G3 strains and estimated mutation rates for Wa-like and DS-1-like time trees. The time to the most common recent ancestors (tMRCA) for G3 strains were estimated in relation to locally circulating human DS-1-like and Wa-like genome segments. The tMRCA and mutation rates were extracted from the time trees generated in Nextstrain for Figure 2 and Supplementary Figure S1.

Genome Segment (Protein)	Wa-like G3P[8]		DS-1-like G3P[4]		Reassortant DS-1-like G3P[4]
	tMCRA (95% CI)	Mutation rates*	tMCRA (95% CI)	Mutation rates	tMCRA (95% CI)
1 (VP1)	21 May 1996 (25 Jul 1990 - 20 Sep 1998)	8.15 x 10 ⁻⁴	11 Feb 2008 (21 Jul 2006 - 10 May 2009)	8.09 x 10 ⁻⁴	12 Feb 2008 (30 Dec 2005 - 15 Feb 2009)
2 (VP2)	03 Jan 2009 (06 Aug 2007 - 06 May 2010)	9.35 x 10 ⁻⁴	18 Oct 2002 (21 Mar 2000 - 15 Mar 2005)	6.43 x 10 ⁻⁴	17 Oct 2002 (24 Nov 1999 - 03 Sep 2004)
3 (VP3) a	12 Jul 2000 (08 Oct 1999 - 11 Nov 2001)	1.04 x 10 ⁻³	05 Jan 2012 (01 Apr 2010 - 22 May 2012)	1.67 x 10 ⁻³	-
4 (VP4)	03 Dec 2008 (14 Nov 2007 - 29 Mar 2010)	8.31 x 10 ⁻⁴	07 Sept 2007 (13 Oct 2003 - 16 Nov 2010)	9.14 x 10 ⁻⁴	28 May 2010 (16 Jul 2006 - 20 Aug 2013)
6 (VP6)	26 Nov 2006 (28 Jun 2003 - 24 Nov 2013)	6.37 x 10 ⁻⁴	14 Dec 2008 (20 Oct 2002 - 18 Nov 2013)	8.30 x 10 ⁻⁴	14 Dec 2008 (20 Oct 2002 - 18 Nov 2013)

5 (NSP1)	15 Mar 2001 (21 Jul 2000 - 17 Jan 2004)	1.55×10^{-3}	15 Jul 2007 (10 Sept 2004 - 17 Jul 2009)	1.44×10^{-3}	15 Jul 2007 (10 Sept 2004 - 17 Jul 2009)
7 (NSP2) b	-	-	17 Jan 2003 (08 Jan 1996 - 28 Jan 2005)	6.59×10^{-4}	-
8 (NSP3)	16 Oct 2005 (10 Jun 2003 - 31 May 2008)	4.23×10^{-4}	21 Jul 2001 (29 Aug 1997 - 10 May 2006)	7.55×10^{-4}	11 May 2009 (13 Jan 2006 - 24 May 2012)
10 (NSP4)	29 Mar 2003 (16 Aug 2000 - 12 Jun 2004)	8.46×10^{-4}	25 Feb 2010 (15 Jul 2005 - 09 Jan 2012)	1.43×10^{-3}	25 Feb 2010 (15 Jul 2005 - 09 Jan 2012)
11 (NSP5)	06 Jan 1995 (19 Nov 1984 - 24 Jun 2001)	2.52×10^{-4}	21 May 2001 (05 Feb 1998 - 25 Jan 2005)	6.09×10^{-4}	21 May 2001 (05 Feb 1998 - 25 Jan 2005)

a. tMRCA were not estimated for reassortant DS-1-like G3P[4] genome segments because they resembled animal-like genome segments thus we could not estimate the correct tMRCA using the current dataset.

b. tMRCA were not estimated for Wa-like NSP2 genome segments due to a lack of a sufficient molecular clock signal to conduct the analysis.

*Mutation rates were defined as the number of substitutions per site per year.